



Hydraulics Research
Wallingford

VALIDATION OF A CURRENT-DEPTH
WAVE REFRACTION COMPUTER MODEL
AGAINST FIELD DATA

C E Jelliman B.Sc

REPORT SR 236
March 1990

Registered Office: Hydraulics Research Limited,
Wallingford, Oxfordshire OX10 8BA.
Telephone: 0491 35381. Telex: 848552

This report describes work carried out by Hydraulics Research under Commission 14D2 funded by the Ministry of Agriculture, Fisheries and Foods, whose nominated officer was Mr A J Allison. At the time of reporting this project, Hydraulics Research's nominated project officer was Dr S W Huntington.

This report is published on behalf of the Ministry of Agriculture, Fisheries and Food, but any opinions expressed are those of the author only, and not necessarily those of the ministry.

© Crown Copyright 1990

Published by permission of the Controller of Her Majesty's Stationery Office.

Validation of a current-depth
wave refraction computer model against field data

Report SR236

March 1990

ABSTRACT

This report describes a validation of a current-depth wave refraction computer model, OUTURAY, which has been developed at Hydraulics Research Limited. The validation concentrated on wave data recorded at Shakespeare Cliff, between Folkestone and Dover. A time series of wave conditions for February 1988 to May 1989 was predicted using the HR HINDWAVE wave hindcasting model. The offshore wave conditions from HINDWAVE were modified using the results from OUTURAY to obtain the wave conditions at the site of the measured data. The predicted wave conditions were compared with the field data. The OUTURAY model was also used without currents for comparison with results from the pure-wave OUTRAY model which ignores current effects and should give identical results. Comparison of the results from OUTURAY with and without current effects indicated the effect that tidal currents had on the waves as they travelled inshore.

The results from OUTRAY and OUTURAY with zero current magnitudes were, as expected, almost identical.

At the Shakespeare cliff waverider site the currents had little effect on the waves at high water but at low water the current effect was significant. At low water the current refracted waves towards the shore normal with wave directions differing by up to 30° of those calculated without taking currents into account. Waves opposing the currents were increased in height by the currents by up to 9% and those from other directions were decreased by up to 50%. Most of the highest waves occurred at high water so the currents did not affect many of the storm peak wave heights. Extreme wave heights were calculated for the separate directional sectors and the results showed that currents had a significant affect on the calculation of rare events. The extremes calculated including currents were up to 9% higher for the direction of the highest waves than those calculated ignoring current refraction. Those in the sectors parallel to the seabed contours were up to 23% lower when current refraction was included in the calculations.

The effect of currents on waves at a point near the entrance to Dover Harbour were quite different from that at the waverider site. The main reason for this was that the current velocities increase as the waves travel from offshore towards the harbour entrance, while they decrease as the waves travel towards the waverider site.

The work described in this report was sponsored by the Ministry of Agriculture, Fisheries and Food.

For further details on this report please contact Miss C E Jelliman or Dr H N Southgate of the Maritime Engineering Department, headed by Dr S W Huntington.

CONTENTS

	Page
1. INTRODUCTION	1
2. DESCRIPTION OF THE COMPUTER MODELS	2
2.1 Introduction	2
2.2 HINDWAVE: The offshore wave prediction model	2
2.3 OUTRAY: The back-tracking refraction model (without currents)	4
2.4 OUTURAY: The back-tracking refraction model including current effects	6
2.5 Linking of HINDWAVE and the refraction models	9
3. VALIDATION OF THE MODELS	10
3.1 Introduction	10
3.2 Setting up and running of the models	11
3.2.1 HINDWAVE	11
3.2.2 OUTRAY	12
3.2.3 OUTURAY	13
3.3 Description of the tidal current data	14
3.4 Sensitivity tests of the OUTURAY model	16
3.4.1 Tests using parallel depth contours and unidirectional currents	16
3.4.2 Tests using depths and currents at Shakespeare Cliff	18
3.5 Results for Shakespeare Cliff	20
4. DISCUSSION	24
5. SUMMARY AND CONCLUSIONS	26
6. ACKNOWLEDGEMENTS	29
7. REFERENCES	30

TABLES

1. H_s ratios for sensitivity tests.
2. Inshore wave directions for sensitivity tests.
3. Distribution of H_s and direction without current effects.
4. Distribution of H_s and direction with current effects.
5. Comparison of storm wave heights.
6. Extreme wave heights.
7. Extreme wave heights for each direction sector.

CONTENTS (CONT'd)

FIGURES

1. Geometry of currents, wave orthogonals and wave rays.
2. Location map
3. Location of refraction grid.
4. Tidal current plot for MHWS.
5. Tidal current plot for 3 hours after MHWS.
6. Tidal current plot for 6 hours after MHWS
7. Tidal current plot for 9 hours after MHWS.
8. Tidal currents for location E1
9. Depth contours and currents for sensitivity tests.
10. Wave heights from sensitivity tests - no currents.
11. Directions from sensitivity tests - no currents.
12. Wave heights from sensitivity tests - with currents.
13. Directions from sensitivity tests - with currents.
14. Wave heights for Feb to May 1988 - no currents.
15. Wave heights for Feb to May 1988 - with currents.
16. Wave heights for June to Sept 1988 - no currents.
17. Wave heights for June to Sept 1988 - with currents.
18. Wave heights for Oct 1988 to Jan 1989 - no currents.
19. Wave heights for Oct 1988 to Jan 1989 - with currents.
20. Wave heights for Feb to May 1989 - no currents.
21. Wave heights for Feb to May 1989 - with currents.
22. Wave directions for Feb to May 1988.
23. Inshore wave rose excluding current effects.
24. Inshore wave rose including current effects.
25. Wave height exceedence curve.
26. Wave height ratios for point 2.
27. Wave directions for point 2.

APPENDICES

1. The HINDWAVE wave hindcasting model.
2. The OUTURAY wave refraction model with currents.
3. Prediction of extreme wave conditions.

1. INTRODUCTION

Hydraulics Research (HR) has many wave refraction models which have been used at sites around the British coast in the last 10 years or more. In recent years wave-current interaction has been introduced into three of these pure-wave computer models, namely the forward-tracking ray model, the back-tracking ray model, and the finite difference model. Each of these pure-wave models caters for different coastal wave prediction problems. The models were tested for some simple cases involving parallel depth contours and unidirectional currents for which analytical solutions are available. These models and tests are described in Reference 1 and they highlighted the need for proper numerical modelling of wave-current problems.

This report describes a validation of one of the HR current-depth refraction models, OUTURAY, a back-tracking ray model. The pure-wave version of this model is called OUTRAY.

Wave conditions were predicted at the site of a waverider buoy about 1.5 km offshore of Shakespeare Cliff, between Dover and Folkestone, based on local wind data from Lydd Ranges. Tidal current information was provided by the TIDEFLOW-2D model (Ref 2) which uses an explicit finite difference method to calculate tidal flows over a gridded area at 10 minute intervals throughout a tidal cycle. The results from OUTURAY were compared with the field wave data. The model was also run with current effects set to zero for comparison with results from the pure-wave OUTRAY model, which should be identical.

Chapter 2 gives a brief description of the models used in this study, with further details given in the appendices. Calibration of the models at a specific

site and the results are described in Chapter 3. A discussion of the results obtained from this study is given in Chapter 4. Finally the conclusions of this study are given in Chapter 5.

2. DESCRIPTION OF THE COMPUTER MODELS

2.1 Introduction

The OUTRAY and OUTURAY back-tracking wave projection models take, as input, wave conditions along the offshore boundary of the model. Therefore, to use the models to predict wave conditions at an inshore site, the corresponding offshore wave conditions are required. In many cases measured wave conditions are not available and it is necessary to use a wave prediction model to obtain them. The HR HINDWAVE wave hindcasting model was used in this study to predict the offshore conditions based on wind data measured at Lydd Ranges. The three mathematical computer models used during this study, HINDWAVE, OUTRAY and OUTURAY are described in this chapter.

2.2 HINDWAVE: The offshore wave prediction model

A common requirement in coastal engineering is to have details of the directional wave climate in deep water offshore. In this study an existing method for wave prediction developed at Wallingford was used. The HINDWAVE model has been used successfully at many points around the UK coast, and has produced good agreement between calculated and measured wave conditions (Ref 3).

The model takes as input details of the geometry of the area in which the waves are generated, and hourly wind records from a local anemometer station (in this case Lydd Ranges). Output from the model is in the form of hourly estimates of wave height, period and direction, which can be condensed into the required probabilistic description of the wave climate.

A detailed description of the HINDWAVE model can be found in Appendix 1 of this report, but briefly the method works as follows. Information about the shape of the wave generation area is presented as a table of fetch lengths, drawn radially outwards at, say, 10° separations from the point of interest. Using this information, and a wave forecasting model based on the JONSWAP method as modified by Seymour (Refs 2 and 3 of Appendix 1), a set of site-specific offshore wave forecasting tables are produced. Each table gives the predicted wave height, period and wave direction for a wide range of wind speeds and directions, assuming a particular (fixed) duration of that wind condition.

A variety of such tables are computed corresponding to a chosen set of durations (in this case 1, 2, 4, 7, 10, 14, 18, 24 and 30 hours). Once the set of forecasting tables has been completed, the second phase of the process begins. At every hour during the period being analysed, the hourly wind records are vectorially averaged over the same number of hours (ie duration) leading up to that hour as were used in setting up the forecasting tables (ie over the preceding 1, 2, 4, ... hours). For each duration, the corresponding wave height is obtained from the relevant table, and the largest of all these values is chosen. This value is stored together with the associated wave period and direction. This procedure is then repeated for the next hour, up to the end of the period of wind data. Once the hourly sequential

wave conditions have been produced it is possible to condense the results into tables giving details of say, the probabilities of particular combinations of wave heights and directions, or wave heights and periods.

There are a number of parameters to be set before using the model, and it is possible to "calibrate" the model by means of slight adjustments to the values of these parameters. Some of the parameters relate to the physics of the model itself, and some to use of land-based wind data to represent conditions over the sea.

2.3 OUTRAY: The back-tracking refraction model (without currents)

The majority of wave generation will occur in deep open expanses of water. Whilst generation will not cease as waves reach shallower water, the effects of the seabed become increasingly important. Wave refraction and shoaling are usually considered together, as both are caused by spatial variations in water depth. Shoaling involves a change in wave height consequent upon the waves slowing down as they travel through water of decreasing depth. Refraction occurs when waves approach the coast at oblique angles of incidence. It involves a gradual change in wave direction as waves travel towards the coast. Both these processes are included in the standard refraction programs used at Hydraulics Research.

Refraction analysis produces sets of transfer functions for wave energy and velocity, dependent upon frequency and direction. These actually take the form of tables of coefficients relating conditions at the

inshore point to those at the offshore point, for each frequency and direction considered. The offshore wave predictions are produced in the form of a directional spectrum, ie an array of energy components as a function of frequency and direction. Each member of the array is multiplied by the appropriate transfer coefficient in order to derive the corresponding inshore spectrum. The spectrum can then be integrated as shown in Appendix 1, in order to calculate the usual parameters, ie significant wave height, mean period and mean direction.

For the refraction analysis, a standard mathematical technique based on the concept of wave rays was used. A full description of the model may be found in Appendix 2 of this report. However, a brief explanation is given here. The technique consists of following or tracking rays seawards from an inshore point to the offshore edge of the grid system. Each ray, which is a line perpendicular to the wave crest, then gives information on how energy travels between the seaward edge of the grid system and the nearshore point of interest. By considering a large number of such ray paths a particular set of matrices may be constructed. This set of matrices are known as transfer functions because they provide a description of the transformation of wave energy between the edge of the refraction grids and the point of interest. Once the transfer functions have been evaluated, and because linear wave theory is being used, the refraction of a large variety of offshore wave conditions can be calculated fairly simply.

An efficient method of combining refraction and HINDWAVE analysis was used in this study, and is described in Section 2.5. A representative sample of wave conditions were put through the refraction procedure, from which the transfer of all other wave

conditions is inferred by interpolation. Refraction calculations were used to transfer wave conditions from the offshore wave prediction point to the nearshore position of interest.

2.4 OUTURAY: The
back-tracking
refraction model
including current
effects

In some areas around the coast the influence of tidal currents on waves is just as important as refraction and shoaling. The effect of currents on the waves depends on the rate of change of the current strength and its direction relative to the wave direction.

In many cases it is advisable to consider the interaction between waves and currents rather than to analyse their separate effects. Significantly different results can be obtained by analysing their interaction, as compared with just simply adding their separate effects. The following simplifications have been made in order to include the effects of wave-current interaction:

1. The effects of waves on currents are ignored. Such effects include rip currents from a beach, and the circulation induced by differences in set-up of the water level between areas of different wave height. Generally the effects of waves on currents are smaller than those of currents on waves and often, as in the case of rip currents, they are localised, small-scale effects.

2. Linear wave theory and the depth refraction approximation are assumed. The latter assumption is that a wave in water of local depth, d , will behave similarly to a wave in water of constant depth, d . This simplification is used in HR's OUTRAY pure-wave model. The reason for this simplification is that it allows currents to be introduced without the equations becoming too complex for the existence of a computational solution in general coastal situations. The refraction approximation does place some limits on the types of waves and bathymetry that can be modelled with reasonable accuracy. Generally the refraction approximation does not hold shorewards of the breaker zone, and will work best where variations in water depth are gradual and regular.
3. The currents are assumed to be vertically uniform and not varying during the time it takes for the waves to reach the inshore location.
4. If the input wave conditions on the offshore boundary have been predicted, they are assumed to include current effects in the wave generation area (ie the area outside the refraction grids). The HR HINDWAVE model assumes current effects are negligible in the wave generation area.

The wave-current OUTURAY model requires gridded values of currents, either as magnitudes and directions or as vector components. The grid system for the currents is the same as that for the depths.

Figure 1 shows the definition of a wave ray. In contrast to pure waves, rays are not directed along orthogonals to wave fronts. Instead they are in the

direction of travel of the absolute group velocity (equal to the vector sum of the current and the relative group velocity). The technique of tracing rays across successive triangular elements is very similar to that used in the pure-wave model. However, there are some differences in the determination of the curvature of the ray paths. In the pure-wave model the wave celerity is assumed to lie on a plane within each triangle. The plane is defined by the values at the corners of the triangle. However, in the wave-current model this is not the case, so the ray paths are not simple circular arcs. The curvature of a ray is calculated as it enters a triangle assuming that the curvature is constant in the triangle. The exit point is determined and the curvature at that point calculated. Knowing the curvatures at the entry and exit point, an estimate can be made of the error in the ray path. If this error exceeds a certain level, the ray path is re-traced using the average of the curvatures at the entry and exit.

The wave height at any position on a ray can be determined by the condition of conservation of wave action along a ray which states:

$$H^2 c_{ga} b / \omega_r = \text{constant} \quad (1)$$

where H is the wave height, c_{ga} is the absolute group velocity, b is the ray separation and ω_r is the relative angular frequency. The term "relative" refers to quantities measured relative to the local current and "absolute" refers to quantities measured relative to the seabed.

Equation (1) can be written in terms of the values of H , c_{ga} , b and ω_r at inshore and offshore locations (referred to by the subscripts o and i);

$$\frac{H_i}{H_o} = (c_{ga_o} / c_{ga_i})^{1/2} (b_o / b_i)^{1/2} (\omega_{r_i} / \omega_{r_o})^{1/2} \quad (2)$$

The variation in wave height due to changes in group velocity is known as shoaling, and the expression $(c_{ga_o} / c_{ga_i})^{1/2}$ is known as the shoaling coefficient.

The expression $(b_o / b_i)^{1/2}$ is known as the refraction coefficient, and $(\omega_{r_i} / \omega_{r_o})^{1/2}$ is known as the Doppler coefficient.

More details on the OUTURAY model are given in Appendix 2.

2.5 Linking of HINDWAVE and the refraction models

HINDWAVE can be combined with each of the OUTRAY and OUTURAY models in a computationally efficient way to simulate a nearshore wave climate at an inshore point. HINDWAVE is used to simulate the wave generation, and OUTURAY or OUTRAY is used to simulate the refraction and shoaling, with or without taking tidal currents into account (respectively).

The first stage of running the HINDWAVE model consists of the transformation of a representative "menu" of wind conditions (expressed as combinations of speed, direction and duration), into a corresponding menu of offshore wave conditions (expressed as significant wave height, mean period and mean direction). A large representative sample of these conditions is turned into directional offshore wave spectra for use with the refraction transfer functions for the inshore point. Each wave condition in the offshore menu can

then be transformed into an equivalent inshore wave condition (with a new significant wave height, mean period and direction). In this way, an inshore wave condition "menu" can be derived for the inshore point, in equivalent format to the offshore menu produced by HINDWAVE.

This retention of the efficient "menu" format for the inshore point allows large quantities of sequential wind data to be processed with quite modest computational effort. Hindcasting of wave conditions for the inshore point is then as simple a matter, and is carried out in the same way, as for the offshore point (see Section 2.2).

3. VALIDATION OF THE MODELS

3.1 Introduction

The site chosen for use in this study was Shakespeare Cliff between Folkestone and Dover. It was chosen because it was one of the few sites where recorded wave data plus detailed tidal current information was readily available. This chapter describes how the OUTURAY and OUTRAY models were used to transform offshore wave conditions predicted by the HINDWAVE model into conditions at a point inshore. The inshore conditions were then compared with the measured data at that point.

Figure 2 gives a general location map for the area of interest. A waverider buoy was situated in about 29m of water, about one and a half kilometres offshore (see Fig 3). It started recording in December 1987 and continued until February 1990. When this study was started wind data was only available for use with

the HINDWAVE model up until the end of May 1989, and so wave data after this month was ignored. Wave data before February 1988 was patchy. So the period of wave data used for simulation in this validation study was February 1988 to May 1989. References 4 and 5 describe the results from a combined HINDWAVE/OUTRAY model ignoring the effects of tidal currents.

3.2 Setting up and running of the models

3.2.1 HINDWAVE

An offshore wave prediction point was chosen near the offshore boundary of the grid system to be used by the refraction models (see Section 3.2.2). It is located due south of the waverider site and 7 km offshore. The position of the offshore point is shown in Figure 3. However, the exact position is not particularly important, as the coastline is so open and the conditions are intended to be representative of the whole offshore boundary of the refraction models.

At this stage, calibration of the models is usually necessary to, for example, adjust the land based wind speeds to those expected over water. In this case, the model had already been calibrated in previous studies at sites nearby using Dungeness wind data (References 4, 6 & 7). Since then the Dungeness weather station has closed down and has been replaced by one at Lydd Ranges (see Fig 2). A study for Shakespeare Cliff (Ref 5) was carried out as a validation of previous work, but using wind data from Lydd Ranges. All of these studies were carried out with the assumption that current effects were

negligible. The calibrated model from these studies was used in this present study.

The wind conditions used to produce the menu of wave conditions were formed from all combination of the values listed below:

directions : 10, 30, 50, ..., 350°N

speeds : 3, 5, ..., 27 m/s

durations : 1, 2, 4, 7, 10, 14, 18, 24 and 30 hours

3.2.2 OUTRAY

The first step in using the OUTRAY and OUTURAY models is to represent the seabed over the area of interest using a set of grids of depth values. Each grid is rectangular and sub-divided into smaller rectangles. A depth value is read off the chart at each corner of these smaller rectangles. The OUTURAY model requires the grid systems for the depths and currents to be identical. The tidal currents already existed in the form of one large grid, so the depths had to be defined by the same grid. Therefore, the grid system used in the previous wave studies for Shakespeare Cliff could not be used. The depth grid used in the HR TIDEWAY two-dimensional modelling system, which computed the tidal currents, was used in the refraction models. The grid is shown on Figure 3. It extends about 14.5 km either side of Shakespeare Cliff to ensure that all waves of importance are modelled. The grid is orientated so that the x-axis makes an angle of 57.75° with North. There are 184 grid points in the x direction and 63 in the y direction, with each grid rectangle being 160m by 160m.

The next step was to choose a set of wave frequencies for use in the ray running program. (The wave frequency (Hz) is simply the inverse of the wave

period in seconds). Although the theoretical basis of the wave refraction method suggests the use of wave frequencies separated by a constant increment, greater computational efficiency can be obtained by using frequencies corresponding to wave periods separated by a constant increment. The periods chosen were 2 to 15 seconds inclusive in 1 second steps, giving a total of 14 wave periods.

For each period an inshore angular ray separation was chosen. Since the shorter period waves do not "feel" the bottom over much of the refraction grid it is possible to use large separations for these waves. On the other hand since longer period waves refract more strongly, a small angular separation is required to give an accurate picture of their refraction behaviour. The following table summarises the angular separations used:

Periods(s)	2-5	6-11	12-15
Separation (°)	1.00	0.50	0.25

It was now possible to run the ray tracing program to produce the transfer function matrices at the site of the waverider. Two sets of transfer functions were obtained, one for MHWS and the other for MLWS. These were then combined with HINDWAVE to produce inshore menus of wave conditions for the two water levels. Times of high water were obtained from Admiralty tide tables. The 16 months of wind data (February 1988 - May 1989) were then run through HINDWAVE and interpolation between the two sets of menus was used depending upon the state of the tide.

3.2.3 OUTURAY

The OUTURAY model was set up and executed in the same way as the OUTRAY model except that a grid of tidal

currents was also input. The current grids were obtained from a previous study (Ref 2) for four stages of the tidal cycle, MHWS and 3, 6 and 9 hours after MHWS. Transfer function matrices were created for these four tidal levels. Four corresponding inshore wave condition menus were produced by HINDWAVE. The 16 months of wind data were then run through HINDWAVE and interpolation between the four sets of menus was carried out to determine the inshore wave conditions.

The OUTURAY model was also run with current magnitudes set to zero for MHWS and MLWS. These were combined with HINDWAVE in the same way as for the transfer function matrices from OUTRAY. The results from OUTURAY with negligible current effects should be identical to those from OUTRAY.

3.3 Description of the tidal current data

The tidal current data was obtained from a previous study for Shakespeare Cliff (Ref 2). It was computed using the TIDEFLOW-2D model, which is formulated on well established equations for the conservation of mass and momentum. Details of the model can be found in Reference 2. Four sets of tidal data were required for this study, for MHWS and 3, 6 and 9 hours after MHWS.

Vector plots of the tidal currents are shown in Figures 4-7. The current velocities and directions near the waverider site, and directly offshore on the offshore boundary of the OUTURAY model, are shown in the table below.

Water level	Offshore		Inshore	
	Velocity (m/s)	Direction (°N)	Velocity (m/s)	Direction (°N)
MHWS	0.95	50	0.81	64
MHWS + 3 hours	0.65	52	0.48	66
MHWS + 6 hours	0.77	233	0.57	248
MHWS + 9 hours	1.07	233	0.35	263

It can be seen in the above table that, in general, the tidal current velocity decreases as the waves travel inshore. The greatest decrease in velocity from offshore to inshore occurs 9 hours after MHWS when it is reduced by about a third. So the greatest effect of the currents on the waves would be expected around this stage of the tidal cycle.

The average tidal cycle at Shakespeare Cliff is about 12 hours 20 minutes. The current meter at station E1 in Reference 2 is only about 250m inshore of the waverider site. The current velocities at E1 reach a maximum about 1 hour after HW. Figure 8 shows the velocity and direction plots for a tidal cycle. The direction of the current is fairly constant, around 65°N, from about 3 hours before HW until about 4 hours after HW. At 4 hours after HW the current velocity drops to about zero and the current direction is reversed. Between 4 hours and 9 hours after HW the tidal current direction gradually changes from 235 to 270°N. About 6 hours after HW the current velocity reaches another maximum though it is almost half as large as the earlier maximum. At 9.5 hours after HW another minimum current velocity occurs. Between 9.5 and 10 hours after HW the tidal current reverses direction again.

3.4 Sensitivity tests of the OUTURAY model

Two sets of tests were carried out using the OUTURAY model to investigate the sensitivity of the model to the offshore wave direction and the current field. One set was for simple depth and current fields and the other was for depth and current fields at Shakespeare Cliff. These tests are described in the sections below.

3.4.1 Tests using parallel depth contours and unidirectional currents

The grid system consisted of one grid with the positive x-axis in an easterly direction. The grid had 10 rows and 25 columns, with each grid element being 30m by 30m. The refraction point was situated approximately in the centre of the ninth row of squares. Six tests were carried out using combinations of 2 depth grids and 3 current fields. One depth grid was for deep water where no depth refraction will occur. The other depth grid has a depth of 15m on the offshore boundary and depths decreasing linearly to 5m on the inshore boundary. The current fields were:

- (1) Zero current velocities (no current refraction will occur). A current field with uniform magnitudes and directions would give the same results.
- (2) Current velocities decreasing linearly from 3m/s offshore to 0.75m/s inshore. All current directions towards 90° N, in the positive x

direction. Figure 9 shows how this current field and the depth field with decreasing depths are defined.

- (3) Current velocities increasing linearly from 0.75 m/s offshore to 3 m/s inshore. All current directions towards 90°N .

All tests were carried out using a single wave period of 16 seconds. Table 1 shows the ratio of the inshore wave height to the offshore wave height for each of the tests. The ratios are the average for each 10° offshore wave direction sector. Table 2 shows the corresponding inshore wave directions for the central direction of each offshore direction sector.

In deep water with uniform currents (test 1) there is no depth or current refraction. So the ray paths are straight and there is no change in wave height along the rays. The shoaling, refraction and Doppler coefficients in equation (2) (Section 2.4) are all equal to unity. In test 2 there was depth refraction but no currents. The waves are refracted towards the shore normal as they travel inshore. The wave heights of the waves travelling normal to the shore (180°N) are not affected by wave refraction but they are increased by shoaling. The shoaling coefficient is 1.56 for all directions. The average refraction coefficient is 0.78 for waves in the sectors 10° either side of the shore normal. The coefficient is lower for larger angles between the wave direction and shore normal because more refraction is occurring. For wave directions $40\text{-}50^{\circ}$ from the shore normal, the average refraction coefficient is 0.70. Test 3 was for waves travelling in deep water (ie no depth refraction) in a direction in which the current velocity is decreasing. For a wave travelling normal to the direction of the current, the wave height and

direction are not significantly changed as it travels along. The greater the angle between the offshore direction and the normal to the current direction the greater the change of wave direction clockwise. The wave height ratio is highest for waves for 200-210°N and lowest for waves from 150-160°N. Test 5 was also for waves in deep water but the current velocity was increasing in the direction the waves travelled. Waves travelling normal to the current direction are unchanged. The greater the angle between wave direction and the normal to the current direction the greater the change in inshore wave direction in an anticlockwise direction. Wave height ratios are highest for 140-150°N and lowest for 200-210°N. Tests 4 and 6 were repeats of 3 and 5 but with linearly decreasing depths.

The test conditions are summarised in Tables 1 and 2 together with the results of the tests. It can be seen from the tables that combining the results from depth refraction only and current refraction only does not give the same results as the tests using both depth and current refraction together.

3.4.2 Tests using depths and currents at Shakespeare Cliff

An offshore directional wave spectrum was created using a single fetch of 100km for all wave directions and the periods used in creating the transfer functions. The offshore significant wave height was 3.6m and the significant wave period was 6.0s. This hypothetical storm was input to the wave transformation models using mean wave directions from 40 to 280°N in 20° increments.

There was no significant difference between the results from the pure-wave OUTRAY model and the

OUTURAY model with current velocities set to zero. This was expected since the OUTURAY model was developed from OUTRAY. If there had been any difference it would have meant an error in one of the models.

Figure 10 shows the offshore to inshore wave height ratio against offshore wave direction for OUTURAY with zero current effects, for MHWS and MLWS. Waves travelling from 150°N offshore are only slightly reduced in height as they travel inshore. The wave height reduction due to refraction and shoaling increases as the offshore wave direction moves away from 150°N. Figure 11 shows the curve of inshore against offshore wave direction. For an offshore wave direction of about 150°N the inshore direction is also about 150°N. Waves from other directions bend towards 150°N as they travel inshore. This is because the normal to the seabed contours seawards of the inshore point is approximately 150°N, and the waves tend to refract towards the normal as they travel inshore. From 140° through to 280°N there is very little difference between the results for high and low waters. Waves with offshore directions from the north east travel through shallower water, so the difference in the amount of wave refraction for the two water levels is greater, with wave heights being about 8% lower at the inshore site for lower water than for high water.

Figures 12 and 13 show the results, including the effects of tidal currents, for the four tidal levels. At MHWS the wave heights are about 1% higher inshore for all directions than those calculated ignoring currents. The wave directions have turned slightly more towards the normal of the seabed contours than in the case without currents. At 3 hours after MHWS the wave directions are fairly similar and the inshore

wave heights only slightly lower than at MHWS. However by 6 hours after MHWS the tide has reversed direction and the curves on Figures 11 and 12 are very different from those for HW. Waves following the current decrease in height as they travel inshore and waves opposing the current increase in height. The inshore directions are nearer 200°N than for MHWS. For the tide 9 hours after MHWS the reduction in wave height is greater than for 6 hours after HW and the wave direction changes less as the waves travel inshore.

3.5 Results for Shakespeare Cliff

The results of the sensitivity tests for the pure-wave OUTRAY model and the OUTURAY model with the zero current velocities were, as expected, not significantly different. Therefore only results from the OUTURAY model are presented in this section. The results consist of predicted hourly wave conditions for February 1988 to May 1989 at the site of the waverider buoy, about 1.5km offshore of Shakespeare Cliff. Two sets of results were predicted, one assuming negligible currents and the other using the real tidal current data.

The combined HINDWAVE and OUTRAY models had been calibrated during previous work assuming that tidal currents were negligible, and using wind data from Dungeness. This weather station has since closed down and has been replaced by one at Lydd Ranges (see Figure 2). The model has not been re-calibrated using wind data from the new station nor taking the effects of tidal currents into account. Therefore the comparison between measurements and predictions may not be as good as it could have been, but it is adequate for this study. In Reference 5 a comparison

between measured waves and waves predicted by the pure-wave OUTRAY model was carried out for the same time period. These predictions were calculated using a different grid system, but in general the results are similar to those obtained from the present study when current velocities are set to zero. Comments on the calibration are given in Reference 5.

Figures 14-21 show comparisons of the measured wave heights against the two sets of predictions, ie with and without current refraction. Some of the measured data was corrupted by interference between 28 November 1988 and 23 January 1989. This data has not been plotted since it was not known which storms were real and which were spurious. The predictions including current effects fluctuate more than those excluding current effects. At high water the two sets of predictions are similar and, since most of the storms occur at high water, most of the storm peaks are similar. One of the most noticeable periods when the two sets of predictions differ is for April 1988 when the inclusion of currents greatly improves the diurnal fluctuations associated with the tides. The predictions including current effects follow the rise and fall of the measured wave height much better than the predictions without currents. Figure 22 gives a comparison of the two sets of predicted inshore wave directions for the first four months. There were no measured directions since the waverider was not a directional recorder. The wave directions predicted taking current effects into account are closer to the beach normal (about 150°N) than those predicted ignoring currents. The two sets of directions are similar for high water but they can differ by about 20 to 30° around low water. Comparison of Figures 14, 15 and 22 show that the difference between the two sets of predicted wave heights is greatest when the waves are from the east.

Tables 3 and 4 show the distribution of wave height and wave direction for the two sets of predictions. The same information is shown in the form of wave roses in Figures 23 and 24. Table 5 shows a comparison of the wave heights for the peaks of storms where either the measured or predicted H_s is over 2m. On average the storm peak wave heights calculated without taking currents into account are 11% underpredicted while those predicted including currents are 8% underpredicted.

Figure 25 shows the wave height exceedence curves for the measured data and two sets of predictions. There is approximately 0.8% of the wave data above a wave height of 2.5m for all three sets of data. Above 1.5m the two sets of predictions have almost identical curves. Below 1.5m there is a greater percentage of the predicted data ignoring currents above a given wave height than for the predicted data including currents. The curve for the wave heights including currents is closer to the curve for the measured data than that without currents. Below 0.5m both sets of predicted wave heights are lower than the measured heights. This may be because only waves travelling from the offshore boundary are modelled, ignoring waves travelling seawards which are locally generated. The waves travelling offshore will only be very small and so are not usually important in wave studies.

Another method of comparing the two sets of predictions is to carry out an extremes analysis to calculate extreme events. This method of analysis is described in Appendix 3. A three-parameter Weibull distribution was fitted to the distribution of H_s for the measured data and both sets of predictions. Extreme significant wave heights were then determined, corresponding to probabilities of three hours occurrence every 1, 10 and 50 years. These results

are listed in Table 6. The extremes calculated from the OUTURAY model results are lower when current effects are excluded. The measured data and the predictions including currents effects lead to similar estimates of extremes, with the predicted 1 in 50 year H_s being about 2% lower than the measured. Without currents the predicted 1 in 50 year H_s is nearly 10% lower than that of the measured data.

The same method of analysis was applied to the wave height data in Tables 3 and 4 to obtain the extremes for each directional sector. These results are listed in Table 7. To the east of 160°N and in the 220-240°N sector the extremes calculated including currents are higher. This is what the sensitivity tests in Section 3.4.2 indicated. From Figures 10 and 12 the waves at MHWS with and without currents were similar. However, at low water the waves from 140-230°N offshore (160-210°N inshore) were higher when current effects were included, and those from other directions were lower than those excluding current effects. In Table 7 the greatest difference between the extreme wave heights predicted with and without currents is 30% for the 1 year return period in the 220-240°N sector, followed by 20% for the same return period in the 60-80°N sector. This is because any of the high wave heights occurring at low water in these sectors when currents are ignored, would be reduced and probably moved into the next sector (80-100 or 200-220°N) when currents are taken into account. For the 1 in 50 year return period, the greatest difference is for waves travelling normal to the coast (120-160°N) where the wave height without currents is 10% greater than the wave height with currents. For the 180-200°N sector the 1 year return period H_s is 8% lower when currents are ignored and the 50 year H_s is 5% lower.

4. DISCUSSION

The OUTRAY and OUTURAY models can be used for nearly any seabed bathymetry provided the depths only vary gently. The models do not include wave breaking, so they would not be applicable where wave breaking occurs. Also, they do not include seabed friction. Generally, waves need to propagate over considerable distances (of the order of kilometres) in shallow water for bottom frictional losses to be significant. In coastal areas where the seabed slopes reasonably steeply to a depth of at least 20m, frictional losses can usually be neglected to a good approximation. The OUTRAY model assumes current refraction is negligible but the OUTURAY model includes the combined effect of current and depth refraction on waves.

The Shakespeare Cliff site chosen for the validation study faces open sea and the seabed is fairly smooth and even. The inshore point is in a depth of about 29m. This is deep enough that wave breaking will not occur, and seabed friction is likely to be insignificant.

The time series of wave predictions were calculated using tidal currents for spring tides for every day of the lunar month. At neap tides the current strengths would be much lower, and hence, the effect of the current on the waves will be less than at spring tide. The differences between the annually averaged results with and without currents are, therefore, likely to be less than that given in Section 3.5. The model could be run using neap tidal currents, if available, as well as spring tidal currents. In many cases it would be sufficient to reduce the magnitudes of the currents at spring tides to give approximate values at neap tides, and for times between these two tides. Offshore of Shakespeare Cliff the strength of the neap

tidal current is about 55% of that of the spring tidal current.

The waverider was situated in an area where current velocities were lower than on the offshore boundary of the refraction models. The current velocities near Dover Harbour, however, are in general higher than those offshore. So the effects of currents on waves are likely to be very different near Dover Harbour than at the waverider site.

In view of this, further runs of the model were carried out to test the sensitivity of the model to the current velocities. The sensitivity tests carried out for the waverider position at Shakespeare Cliff (Section 3.4.2) were also carried out for a point near the entrance to Dover Harbour for low and high water.

Figure 26 shows the offshore to inshore wave height ratios and Figure 27 shows the mean inshore wave angles as a function of offshore wave direction for a point near Dover Harbour. These curves are very different from the equivalent curves at the waverider site in Figures 12 and 14. At the waverider position the effect of currents on wave heights was only small at high water. At low water waves from the east were reduced by the currents and those from the south were increased. Near the entrance to Dover Harbour, however, the effect of current refraction on wave heights at high water was to increase waves from 20-200°N. Wave heights for an offshore direction of 80°N were about doubled when current refraction was taken into account. At low water the currents only slightly increased the waves from 20-160°N and waves from 160-260°N were decreased by up to 10% of their offshore height.

Figure 2.8 of Reference 8 gives an equation for calculating the effect a current has on the wave height. However, this equation is for waves travelling from still water into a steadily increasing current velocity in deep water. So it is not suitable for use when the waves are travelling into a decreasing current velocity or when the offshore current is not negligible. It also ignores the interaction between current and depth refraction. Sometimes tidal current data is only available for one or two points inshore, such as that given by Admiralty Diamond tidal stream data. If the currents are negligible offshore and they can be assumed to be increasing linearly in the inshore direction then the equation in Reference 8 could be used to give a rough indication of the effect the current has on the wave height. Figure 2.7 of Reference 8 gives an indication of maximum tidal currents around the coast of Great Britain.

5. SUMMARY AND CONCLUSIONS

This report has considered the transformation of wave energy from offshore to an inshore site using HR's OUTURAY current-depth wave refraction model. The model was validated using field wave data and tidal current data from the HR TIDEWAY-2D model for an area offshore of Shakespeare Cliff, near Dover.

The OUTURAY model was first run with current velocities set to zero so that it could be checked against the pure-wave OUTRAY model. The two models gave identical results. Next some tests were carried out using simple depth and current fields. These tests showed that the depth and current refraction should not be considered separately since their

interaction was important. They also highlighted the need for proper numerical modelling of wave-current problems.

The HR HINDWAVE model was used to simulate hourly wave data at an offshore site for the period February 1988 to May 1989. These were then transformed by OUTURAY into conditions at the site of a waverider buoy 1.5km offshore from Shakespeare Cliff. Two sets of predictions were calculated, one without current refraction and one with. Both sets were compared with wave data recorded by the waverider. At high water the currents had little effect on the waves, only increasing heights by 1%. But at low water waves from 160-230°N offshore were increased by up to 10% by current refraction, whilst those from the east were nearly halved. The inshore wave directions were closer to the beach normal (150°N) at low water when current effects were included than when they were ignored. At high water, current refraction hardly affected the wave directions. Many of the storm peaks occurred at high water when the currents had little effect. For those storms including significant wave heights above 2m, the peak wave heights ignoring currents were underpredicted on average by 11% and those calculated including current effects were underpredicted on average by 8%.

Extreme wave heights were derived from the measured data and from the two sets of predicted data. Those from the predictions including currents were similar to those from the measured data, with the predicted once in 50 year wave height being only 2% lower. The extremes from the predictions without currents were lower than those from the measurements by up to 10%. (This does not necessarily imply a 10% error in the original prediction work done for Shakespeare Cliff, since then a different grid system was being used and

wind data from Dungeness was used instead of that from Lydd Ranges). Extremes were also calculated for separate directional sectors between 60 and 240°N. These were quite different for the two sets of predictions. The extremes were up to 9% higher for the direction of the highest waves, SSW, when current effects were included and up to 23% lower for the directions parallel to the seabed contours. The tidal current data used in the model was for spring tides only. During neap tides, when the current strength is smaller, the effect of currents on the waves will have been over-predicted by the model. Therefore, the annually averaged differences between the two sets of wave data, with and without currents, will be less than that quoted above.

In general, the inclusion of current effects in the model improved the wave predictions and had a significant effect in the calculation of rare events. It also made a difference to the wave directions which may be important if the data is to be used for the calculation of coastal sediment transport.

The effect of currents on the waves was very different near Dover Harbour than at the waverider site. One reason for this is that the current velocities increase as waves travel towards the harbour while they decrease as waves travel towards the waverider.

The calculation of current-depth refraction is complicated. Therefore it is not easy to tell whether current refraction has any effect on waves at a given site without using the model, unless the current velocities are small enough to be negligible.

6. ACKNOWLEDGEMENTS

This study was carried out by Miss C E Jelliman of Dr A H Brampton's Coastal Processes Section at Hydraulics Research. This section is part of the Maritime Engineering Department, headed by Dr S W Huntington. The author would like to thank Dr H N Southgate and Dr P J Hawkes for advice during this study. Mr T J Chesher and Dr G V Miles of the Tidal Engineering Department are thanked for providing the tidal current data.

Thanks are due to Mr Rod Davis of the Meteorological Office for supplying the wind data.

Thanks are due to Transmanche-Link for permission to use the Shakespeare Cliff wave data in the validation work, and to present the results in this report.

7. REFERENCES

1. Southgate H N. Current-depth refraction of water waves - a description and verification of three numerical models. HR Report No SR 14, January 1985.
2. Marine works at Shakespeare Cliff - Sediment transport study. HR Report EX 1585, September 1987. Confidential to Transmanche-Link.
3. P J Hawkes. A wave hindcasting model. Modelling the offshore environment, Society for Underwater Technology, April 1987.
4. The Channel Tunnel Project, Wave studies at Shakespeare Cliff, Dover, Vol I. HR Report EX 1501, November 1986. Confidential to Transmanche-Link.
5. Validation of wave direction predictions at Shakespeare Cliff - Final report. HR Report EX 2111. (In preparation). Confidential to Transmanche-Link.
6. Seaford Frontage Study - Data collection and analysis. HR Report EX 1345, September 1985. Confidential to Southern Water Authority.
7. Dover Harbour, A random wave model investigation. HR Report EX 1275, March 1985. Confidential to Dover Harbour Authority.
8. Report of the Environmental Conditions Committee of the International Ship Structures 6th Congress, Boston, 1976.

Tables

TABLE 1 : H_s ratios for sensitivity tests

The table below shows the average ratio of the offshore to inshore wave height in each direction sector for a single period of 16 seconds.

Test Number	1	2	3	4	5	6
Currents*	C	C	D	D	I	I
Depths [‡]	Deep	Lin	Deep	Lin	Deep	Lin
Offshore Wave Direction (°N)						
130-140	1.000	1.091	1.027	1.005	1.003	1.147
140-150	1.000	1.145	0.975	1.073	1.028	1.198
150-160	1.000	1.184	0.969	1.118	1.027	1.217
160-170	1.000	1.223	0.978	1.177	1.013	1.226
170-180	1.000	1.223	0.990	1.213	1.010	1.237
180-190	1.000	1.223	1.003	1.245	0.991	1.216
190-200	1.000	1.223	1.024	1.256	0.982	1.192
200-210	1.000	1.184	1.027	1.239	0.969	1.147
210-220	1.000	1.145	1.021	1.223	0.981	1.096
220-230	1.000	1.091	1.008	1.173	0.776	1.043

* Currents to the east

C - Constant currents

D - Currents decreasing towards the shore

I - Currents increasing towards the shore

[‡] Depths

Deep - Deep water, ie no depth refraction

Lin - Decreasing linearly towards the shore

TABLE 2 : Inshore wave directions for sensitivity tests

Test Number	1	2	3	4	5	6
Currents*	C	C	D	D	I	I
Depths [‡]	Deep	Lin	Deep	Lin	Deep	Lin
Offshore Wave Direction (°N)						
135	135	154	126	149	141	157
145	145	159	140	156	149	162
155	155	165	153	163	157	166
165	165	171	164	170	166	171
175	175	177	175	176	175	177
185	185	183	185	183	185	183
195	195	189	194	188	196	190
205	205	195	203	194	207	197
215	215	201	212	198	219	203
225	225	206	219	202	230	210

* Currents to the east

C - Constant currents

D - Currents decreasing towards the shore

I - Currents increasing towards the shore

[‡] Depths

Deep - Deep water ie no depth refraction

Lin - Decreasing linearly towards the shore

TABLE 3 : Distribution of Hs and direction without current effects

Waverider buoy location , 1.5 km offshore of Shakespeare Cliff

Predicted wave conditions for February 1988 to May 1989

Data in parts per hundred thousand

Significant wave height in metres

H1	To H2	P(H>H1)	Wave angles in degrees North										
			40	60	80	100	120	140	160	180	200	220	240
			60	80	100	120	140	160	180	200	220	240	260
0.00	0.25	0.9568	163	7056	1132	257	146	154	163	429	1595	6464	489
0.25	0.50	0.7763	0	3995	4278	1157	514	480	1097	1149	4973	2743	0
0.50	0.75	0.5724	0	1509	2769	574	343	429	617	1569	4904	2203	0
0.75	1.00	0.4233	0	283	1260	214	60	214	703	2015	7339	1500	0
1.00	1.25	0.2874	0	737	2006	291	9	0	171	686	6036	1183	0
1.25	1.50	0.1762	0	300	437	0	0	0	86	1200	3018	1200	0
1.50	1.75	0.1138	0	0	180	0	0	0	0	377	4081	686	0
1.75	2.00	0.0605	0	0	86	0	0	0	43	737	1663	171	0
2.00	2.25	0.0335	0	0	0	0	0	0	0	257	995	171	0
2.25	2.50	0.0193	0	0	0	0	0	0	0	154	986	34	0
2.50	2.75	0.0075	0	0	0	0	0	0	0	103	163	0	0
2.75	3.00	0.0049	0	0	0	0	0	0	0	0	343	43	0
3.00	3.25	0.0010	0	0	0	0	0	0	0	0	103	0	0
Parts per thousand For each direction			2	145	127	26	11	13	30	91	378	171	5

TABLE 4 : Distribution of Hs and direction with current effects
Waverider buoy location , 1.5 km offshore of Shakespeare Cliff
Predicted wave conditions for February 1988 to May 1989
Data in parts per hundred thousand
Significant wave height in metres

H1 To H2	P(H>H1)	Wave angles in degrees North											
		40	60	80	100	120	140	160	180	200	220	240	
		60	80	100	120	140	160	180	200	220	240	260	
0.00	0.25	0.9559	26	2323	7150	2563	617	643	1252	2666	4424	3121	26
0.25	0.50	0.7068	0	900	4535	2555	617	626	1818	4227	4252	763	0
0.50	0.75	0.5039	0	317	2786	960	274	574	960	3652	3575	360	0
0.75	1.00	0.3693	0	154	1252	403	120	120	892	3918	5067	231	0
1.00	1.25	0.2477	0	129	686	103	9	0	146	2726	4510	111	0
1.25	1.50	0.1635	0	60	257	0	0	0	137	1800	2452	291	0
1.50	1.75	0.1135	0	0	51	0	0	0	0	1740	3361	103	0
1.75	2.00	0.0610	0	0	51	0	0	0	34	1175	1483	9	0
2.00	2.25	0.0334	0	0	0	0	0	0	0	660	703	0	0
2.25	2.50	0.0198	0	0	0	0	0	0	0	677	574	0	0
2.50	2.75	0.0073	0	0	0	0	0	0	0	197	257	0	0
2.75	3.00	0.0027	0	0	0	0	0	0	0	0	163	9	0
3.00	3.25	0.0010	0	0	0	0	0	0	0	9	94	0	0
Parts per thousand For each direction			0	41	175	69	17	21	55	245	323	52	0

TABLE 5 : Comparison of storm wave heights

Location: Site of the waverider buoy, 1.5km offshore of Shakespeare Cliff

Date	Wave Height (m)					Predicted Wind Direction (°N)
	Measured H_s	Predicted H_s (NC) H_s (C)		H_s (NC)/ H_s	H_s (C)/ H_s	
1-2/2/88	3.2	3.2	3.2	1.02	1.02	210
4/2/88	2.5	2.4	2.5	0.93	0.98	220
8/2/88*	2.9	1.6	1.6	0.55	0.55	230
8-10/2/88	2.4	1.9	1.9	0.78	0.79	240
13-14/2/88	2.7	2.4	2.7	0.89	1.02	190
3/3/88	2.0	1.3	1.3	0.67	0.65	230
20/3/88	2.1	1.0	0.9	0.49	0.44	260
4/7/88	1.9	2.3	2.5	1.22	1.29	210
25-26/7/88	1.8	2.3	2.3	1.32	1.32	220
19/8/88	2.2	2.0	1.9	0.91	0.87	240
31/8/88	2.0	1.9	1.9	0.92	0.95	220
1-3/9/88	2.5	2.3	2.4	0.92	0.96	210
23/9/88*	3.4	1.7	1.8	0.50	0.51	240
24/9/88	2.3	1.6	1.5	0.68	0.66	260
26/9/88	2.2	1.6	1.6	0.73	0.74	250
28/9/88	2.6	2.4	2.3	0.91	0.87	240
6/10/88	2.4	1.6	1.5	0.66	0.64	240
7/10/88	2.3	1.6	1.6	0.68	0.69	260
8-10/10/88	3.0	2.8	2.8	0.93	0.93	240
12-13/10/88	2.2	1.8	2.0	0.80	0.91	190
4-5/2/89	2.1	2.0	2.0	0.98	0.96	230
18-19/2/89	2.3	2.3	2.5	1.02	1.08	200
24-25/2/89	2.5	1.8	2.1	0.71	0.82	170
9-10/3/89	1.6	2.2	2.5	1.37	1.55	190
14-15/3/89	2.9	2.6	2.7	0.88	0.92	200
18-20/3/89	1.7	2.3	2.5	1.35	1.43	210
22-23/3/89	2.2	2.0	2.0	0.90	0.90	230
23-25/3/89	2.7	3.0	3.2	1.12	1.18	220
4/4/89	2.1	1.2	1.2	0.56	0.55	30
11-12/4/89	2.5	2.6	2.7	1.03	1.09	200
12/5/89	1.9	2.0	2.1	1.10	1.11	240
		Average ratio		0.89	0.92	

H_s (NC) - wave height calculated ignoring currents.

H_s (C) - wave height calculated including currents.

* Short duration storm.

TABLE 6 : Extreme wave heights

Location: Site of waverider buoy, 1.5km offshore of Shakespeare Cliff

Extreme significant wave heights in metres calculated assuming 3 hourly events.

Return period (years)	From measured data*	From OUTURAY Model*	
		without currents	with currents
1	3.46	3.32	3.46
10	4.14	3.86	4.08
50	4.59	4.19	4.48

*Predictions and measurements for 28/11/88 to 23/1/89 were not included in the analysis because some of the measured data was spurious.

TABLE 7 : Extreme wave heights for each direction sector

Location: Site of waverider buoy, 1.5km offshore of Shakespeare Cliff

Extreme significant wave heights in metres calculated assuming 3 hourly events.

Centre of inshore wave direction sector	Return period (years)					
	1		10		50	
	NC*	C*	NC*	C*	NC*	C*
70	1.52	1.27	1.89	1.74	2.13	2.04
90	1.81	1.68	2.12	2.06	2.30	2.31
110	1.17	1.08	1.44	1.31	1.59	1.45
130	0.85	0.88	1.17	1.11	1.37	1.24
150	0.99	0.90	1.17	1.07	1.27	1.16
170	1.59	1.60	2.03	2.03	2.30	2.30
190	2.91	3.17	3.53	3.75	3.91	4.12
210	3.24	3.27	3.73	3.80	4.03	4.13
230	2.54	1.95	3.11	2.72	3.46	3.23

* NC - Current effects not included in hourly predictions.

C - Current effects included.

Figures

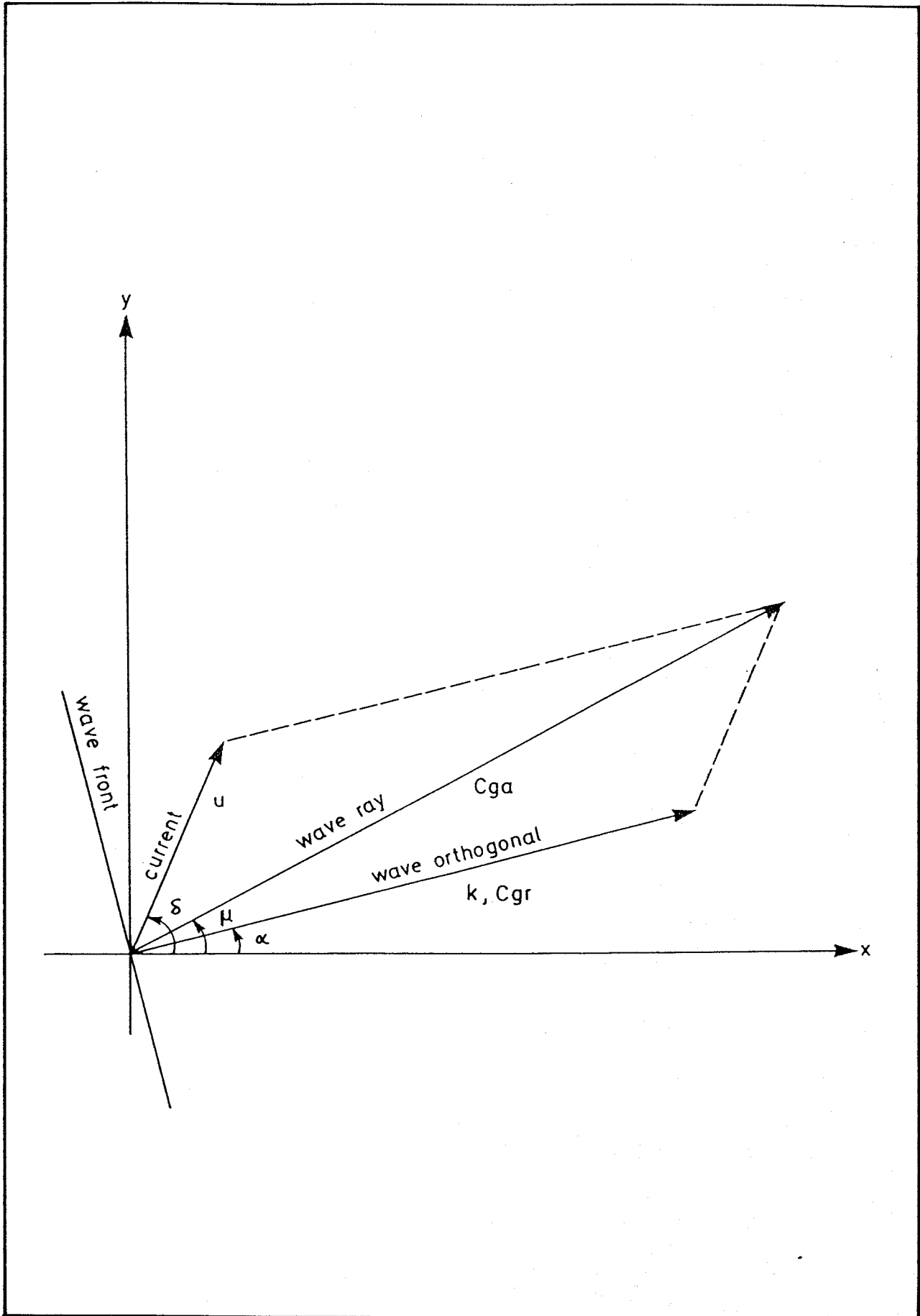


Fig 1 Geometry of currents, wave orthogonals and wave rays.

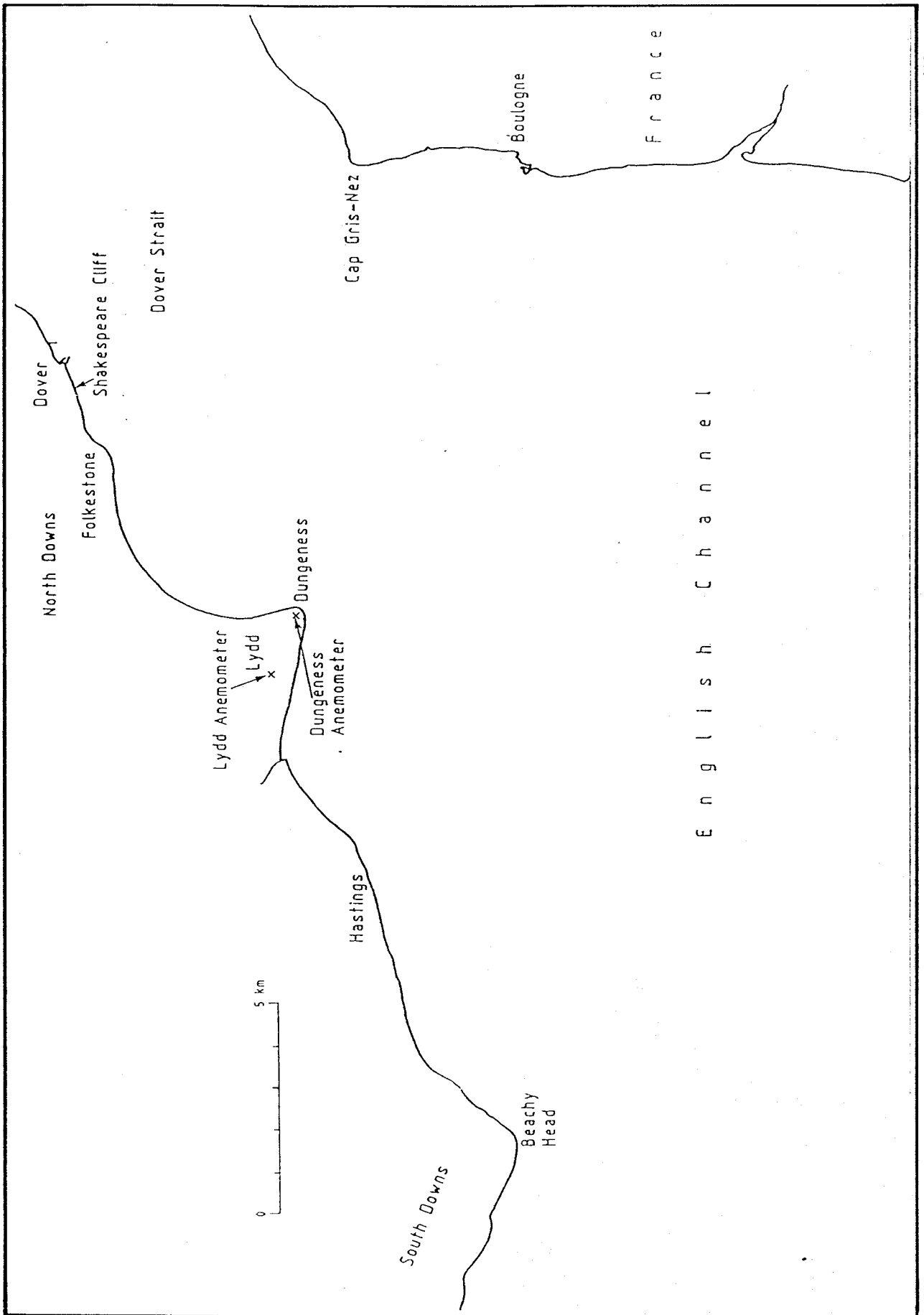


Fig 2 Location map.

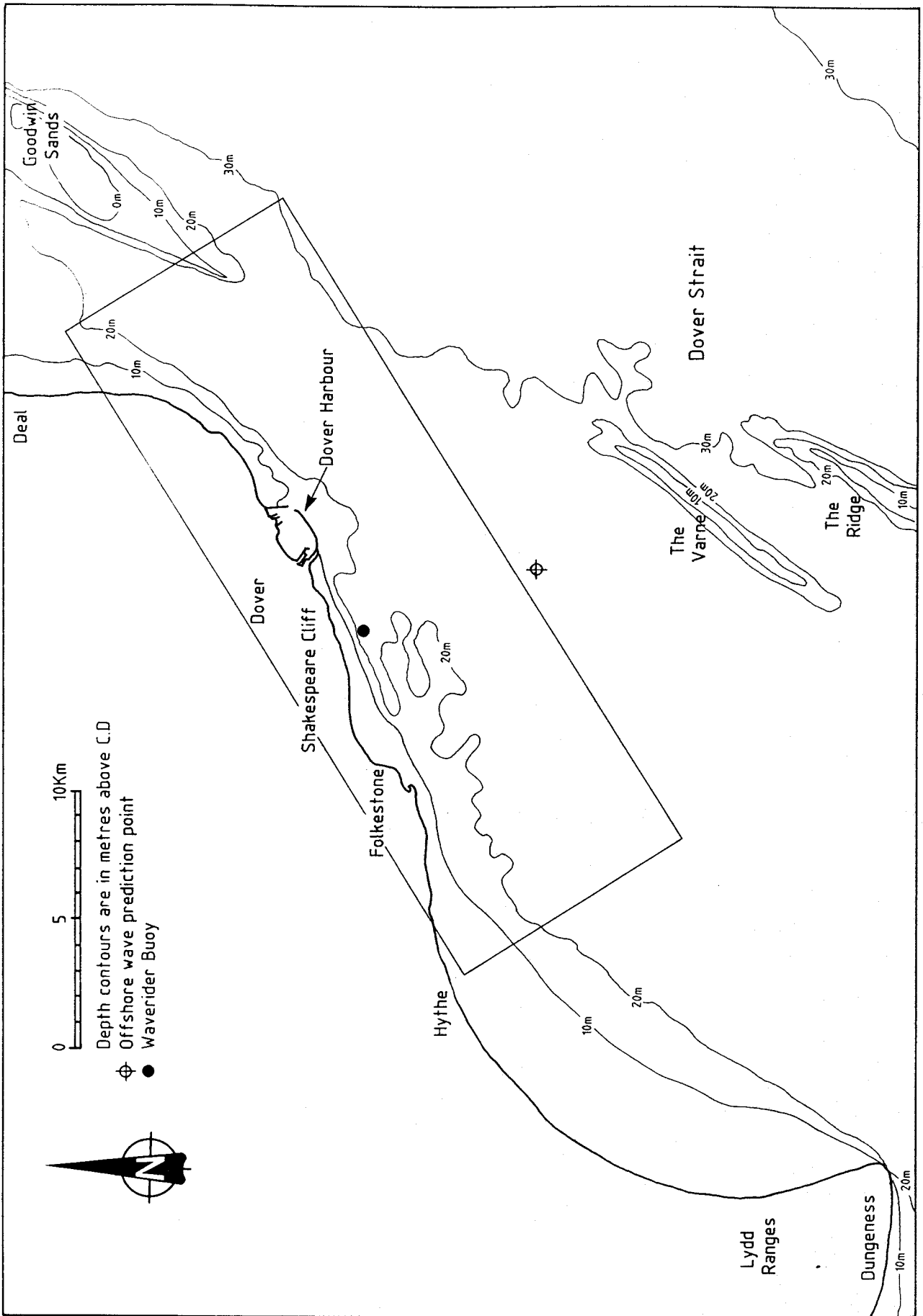


Fig 3 Location of refraction grid.

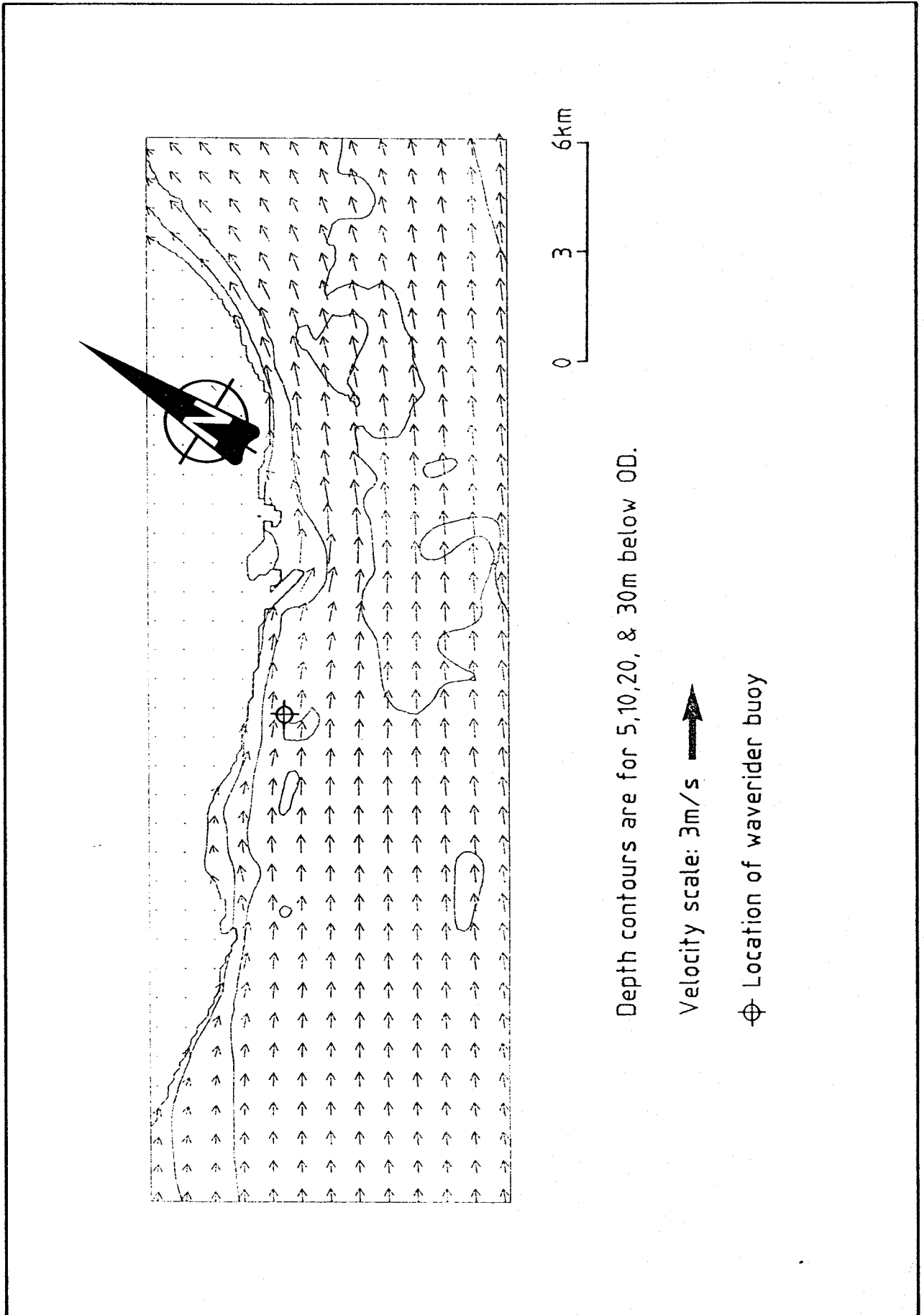


Fig 4 Tidal current plot for MHWS.

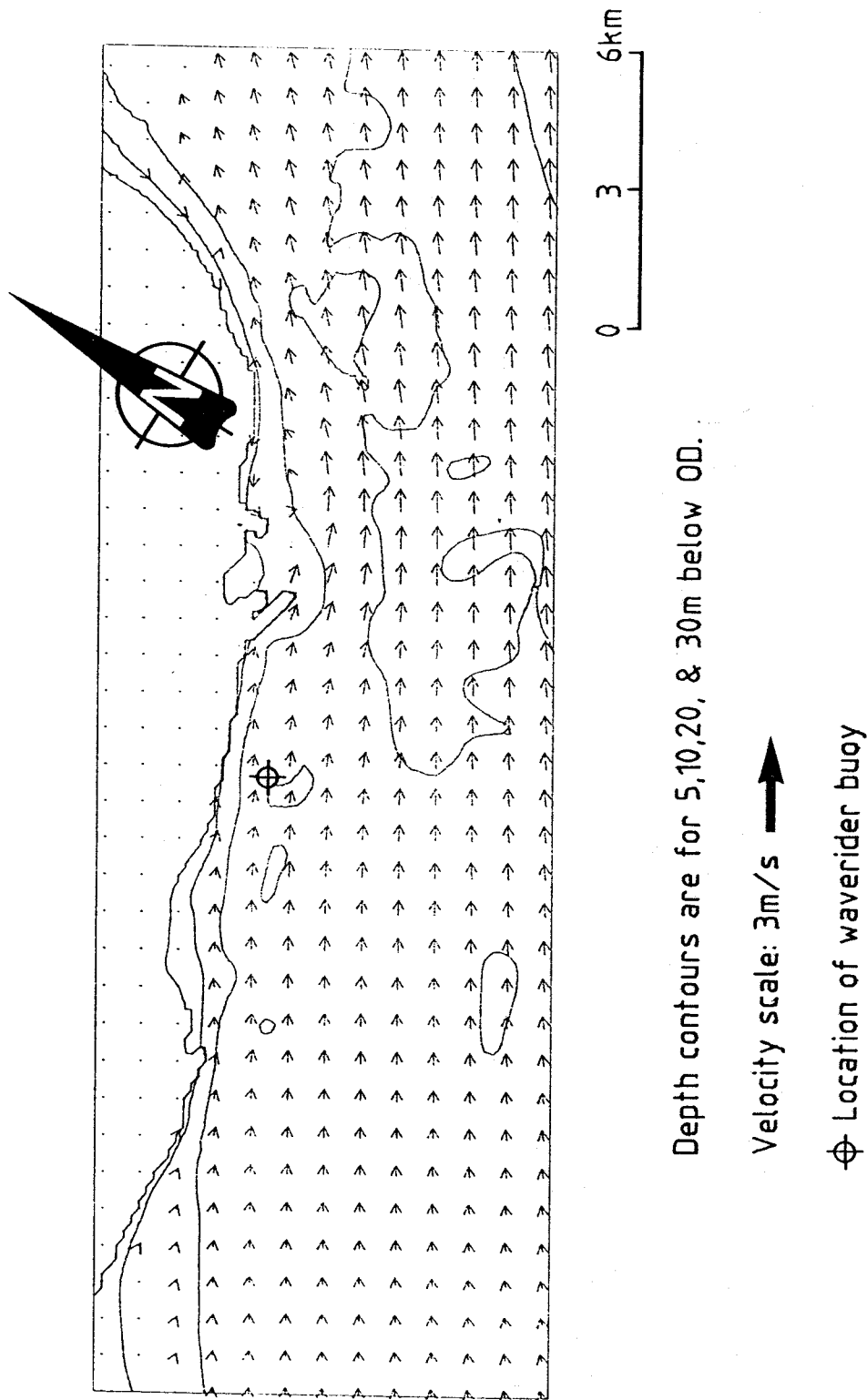


Fig 5 Tidal current plot for 3 hours after MHWS.

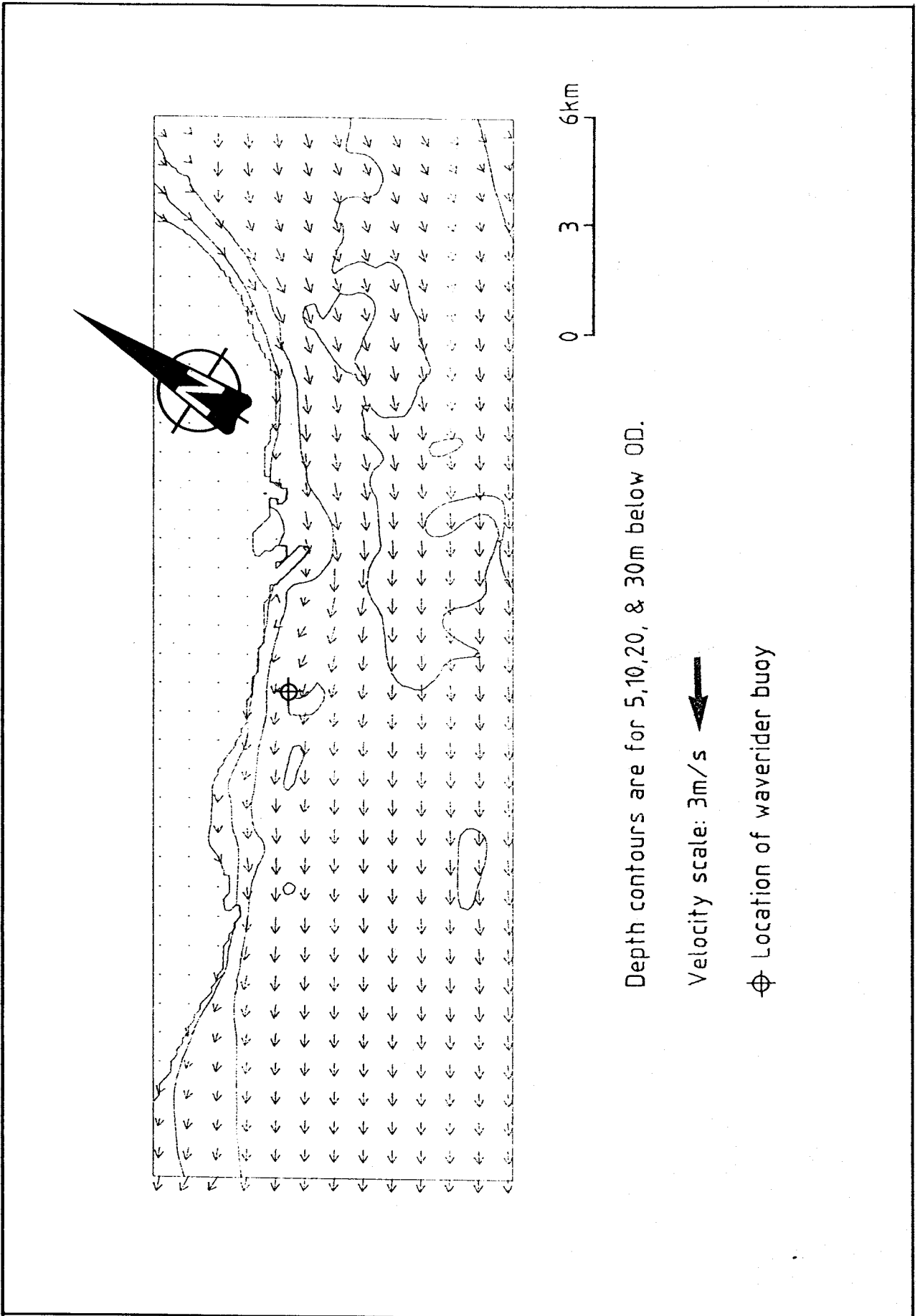


Fig 6 Tidal current plot for 6 hours after MHWS.

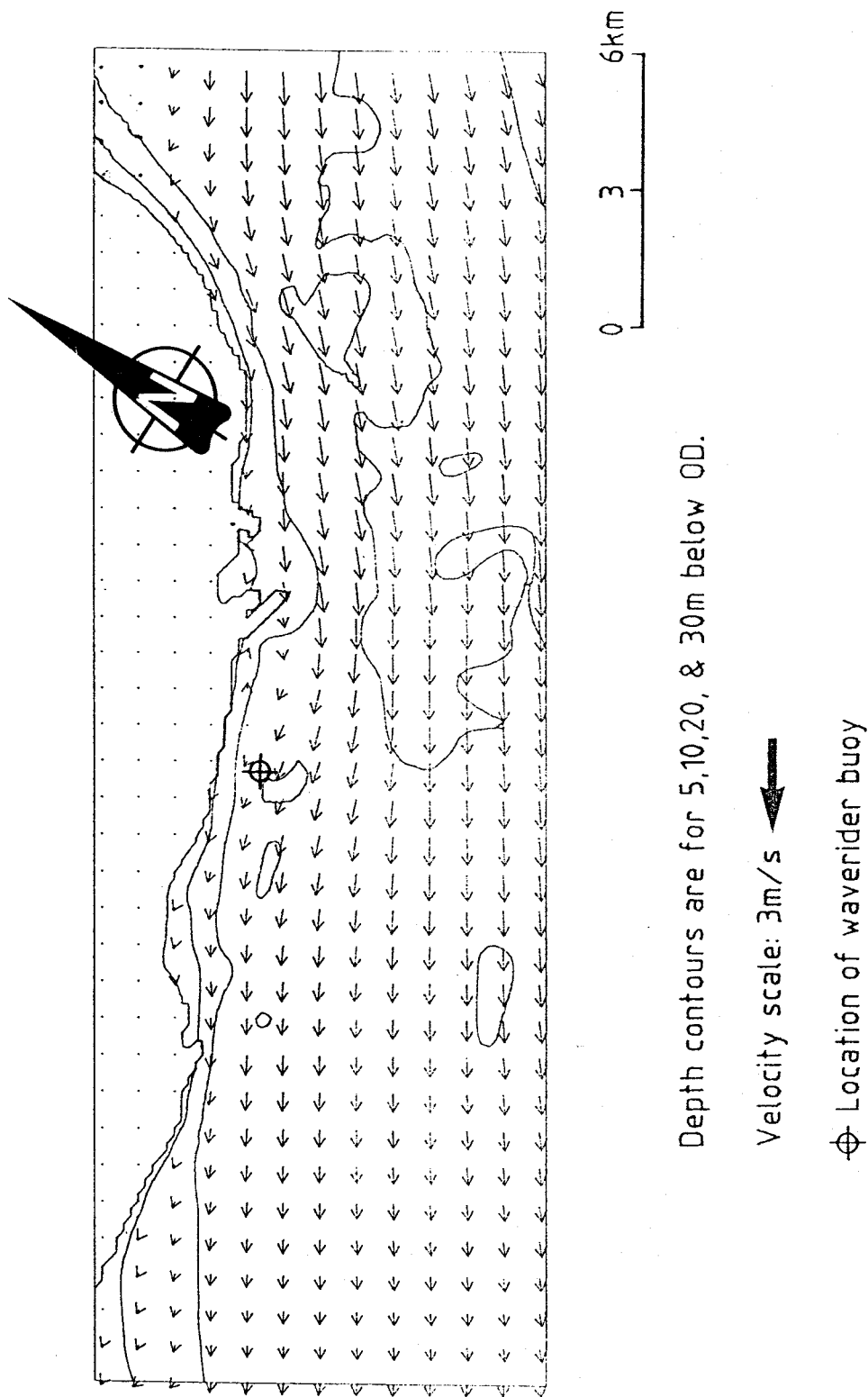


Fig 7 Tidal current plot for 9 hours after MHWS.

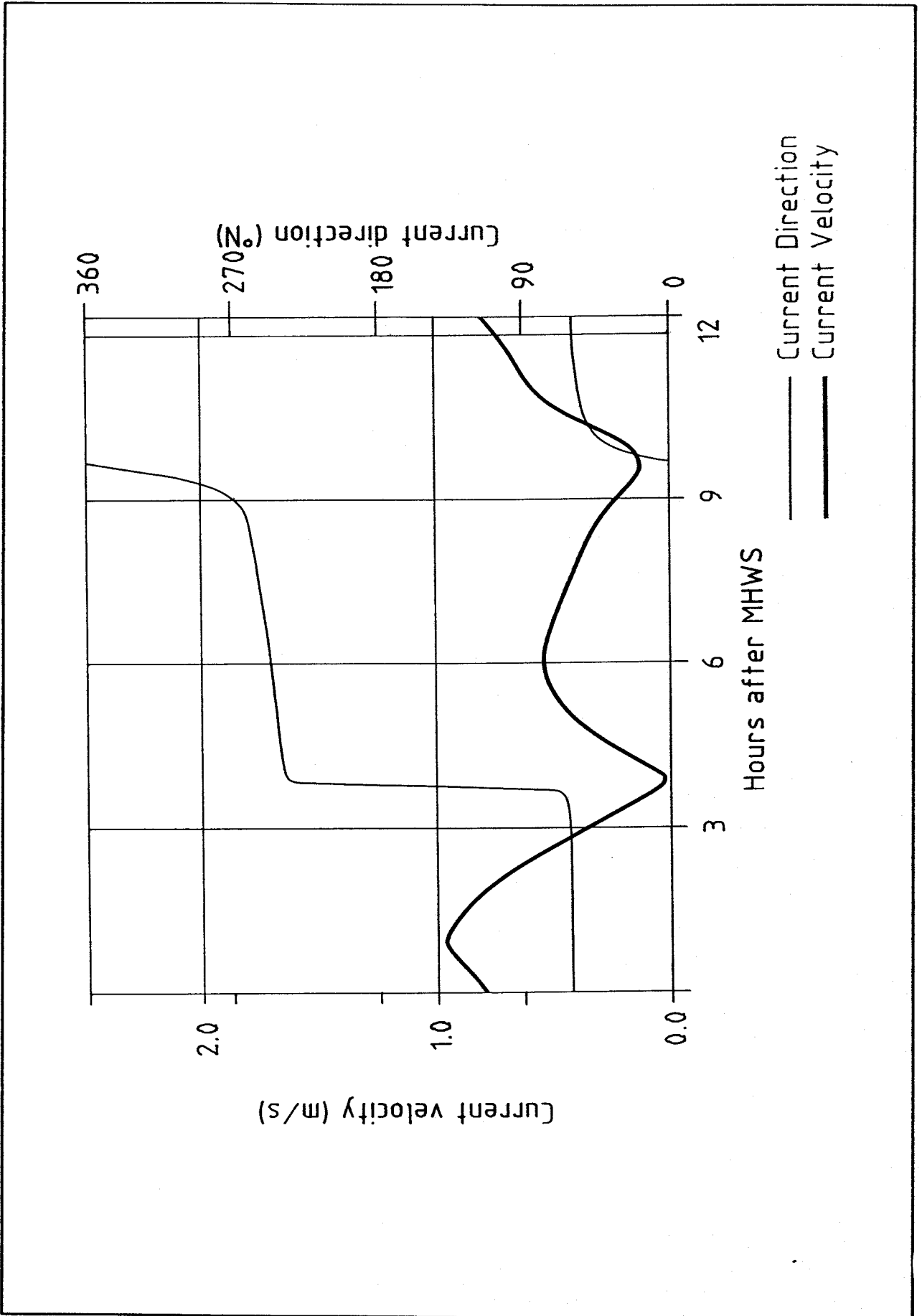


Fig 8 Tidal currents for location E1.

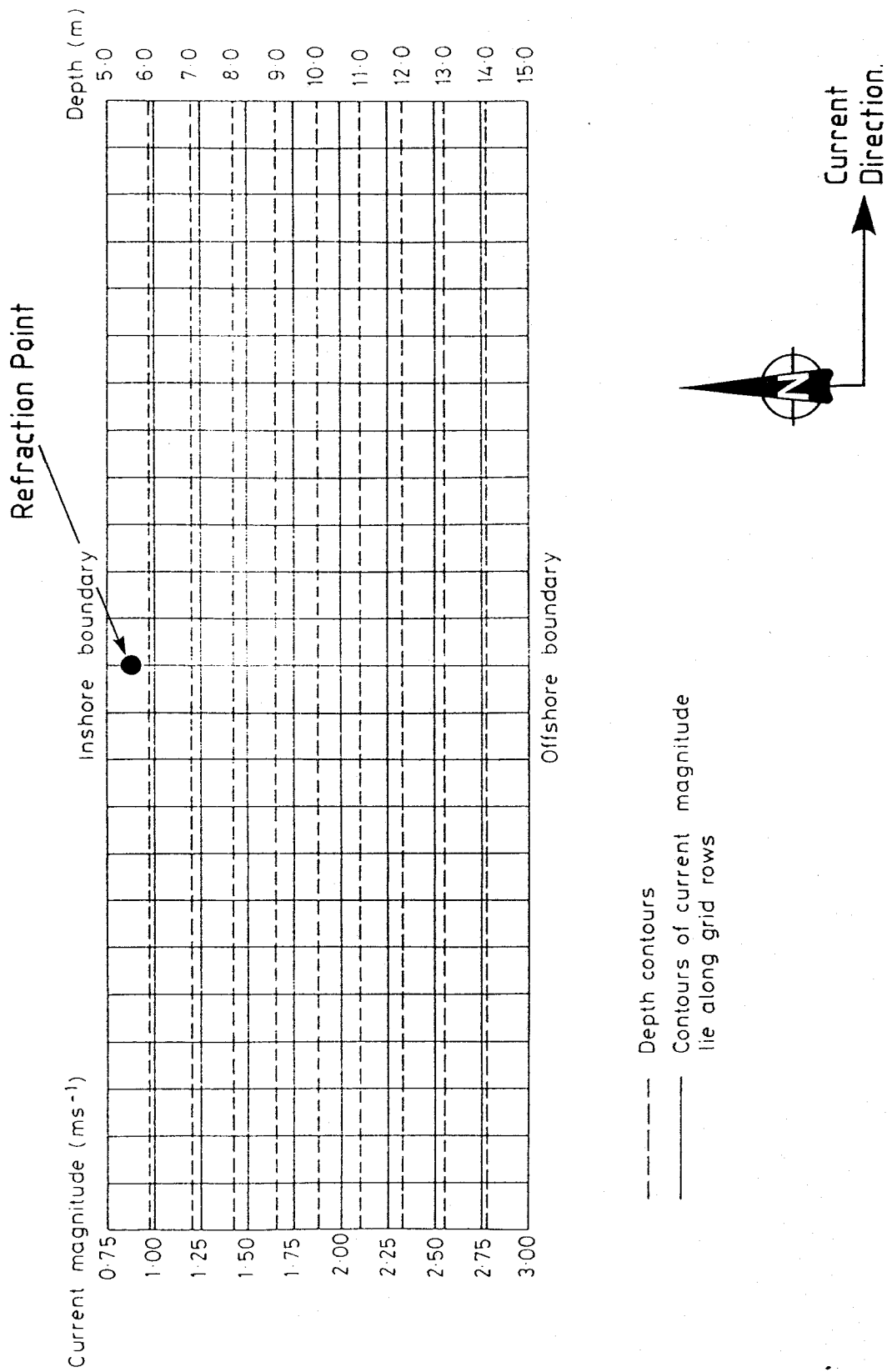


Fig 9 Depth contours and currents for sensitivity tests.

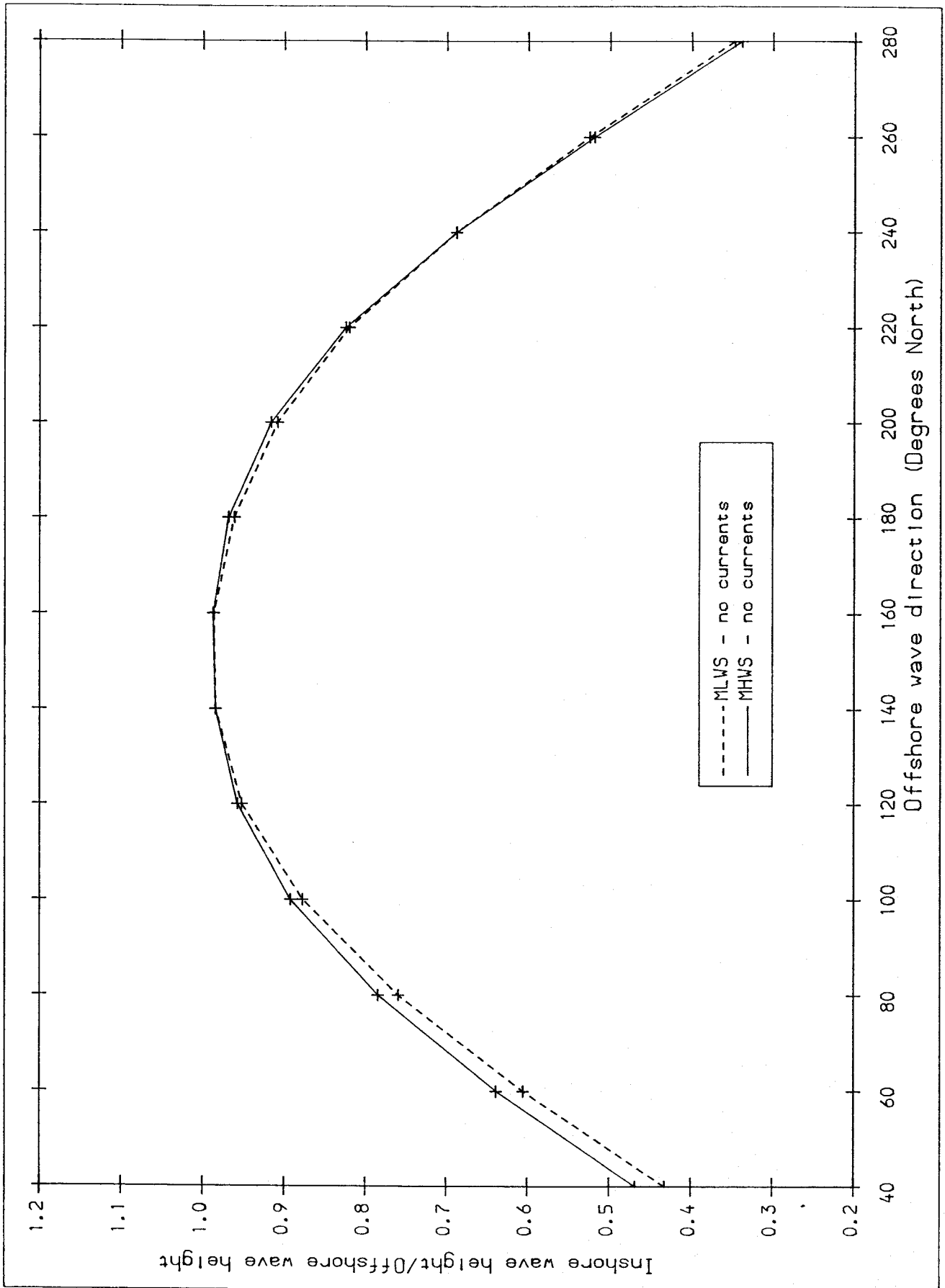


Fig 10 Wave heights from sensitivity tests - no currents

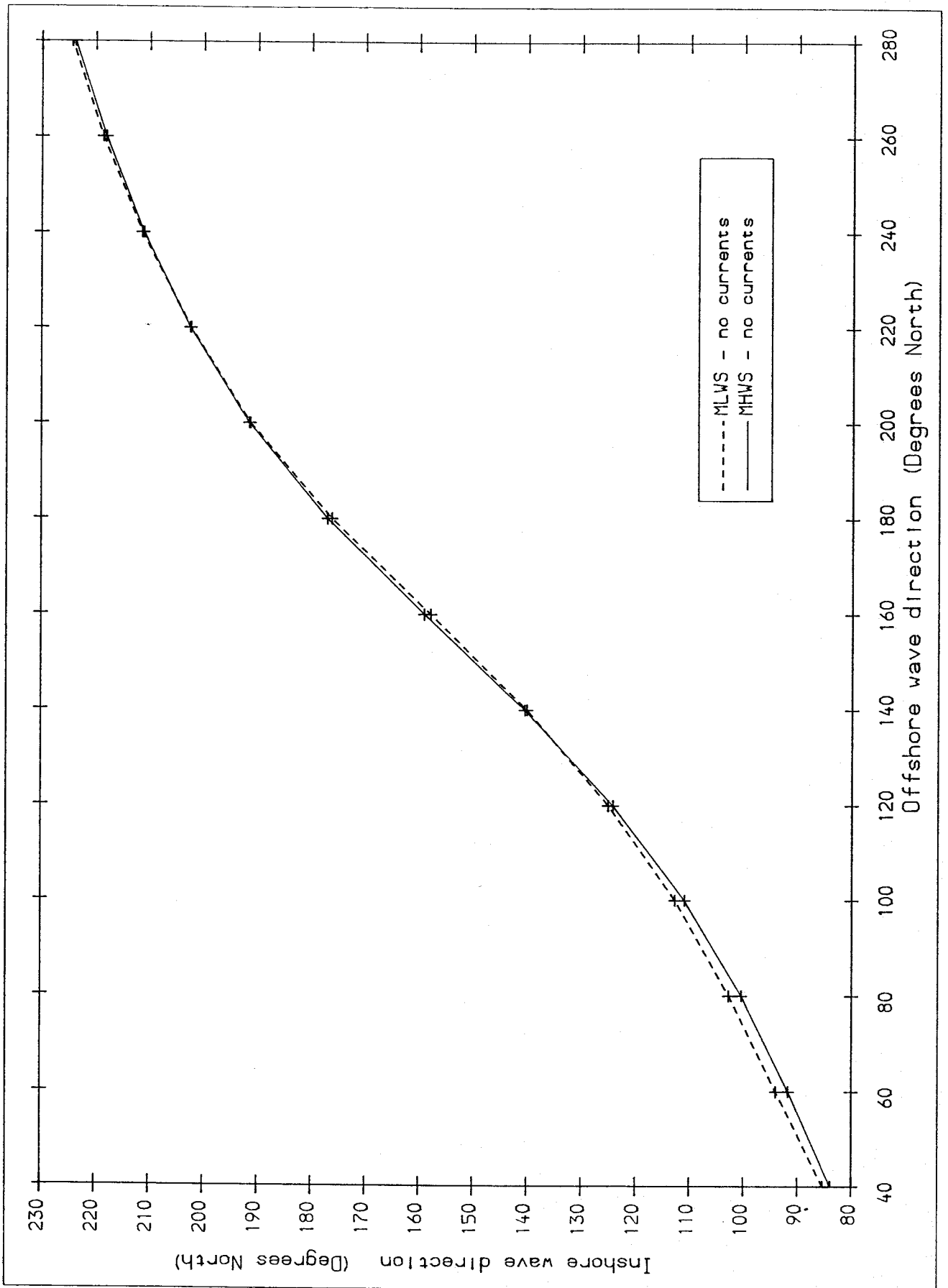


Fig 11 Directions from sensitivity tests - no currents

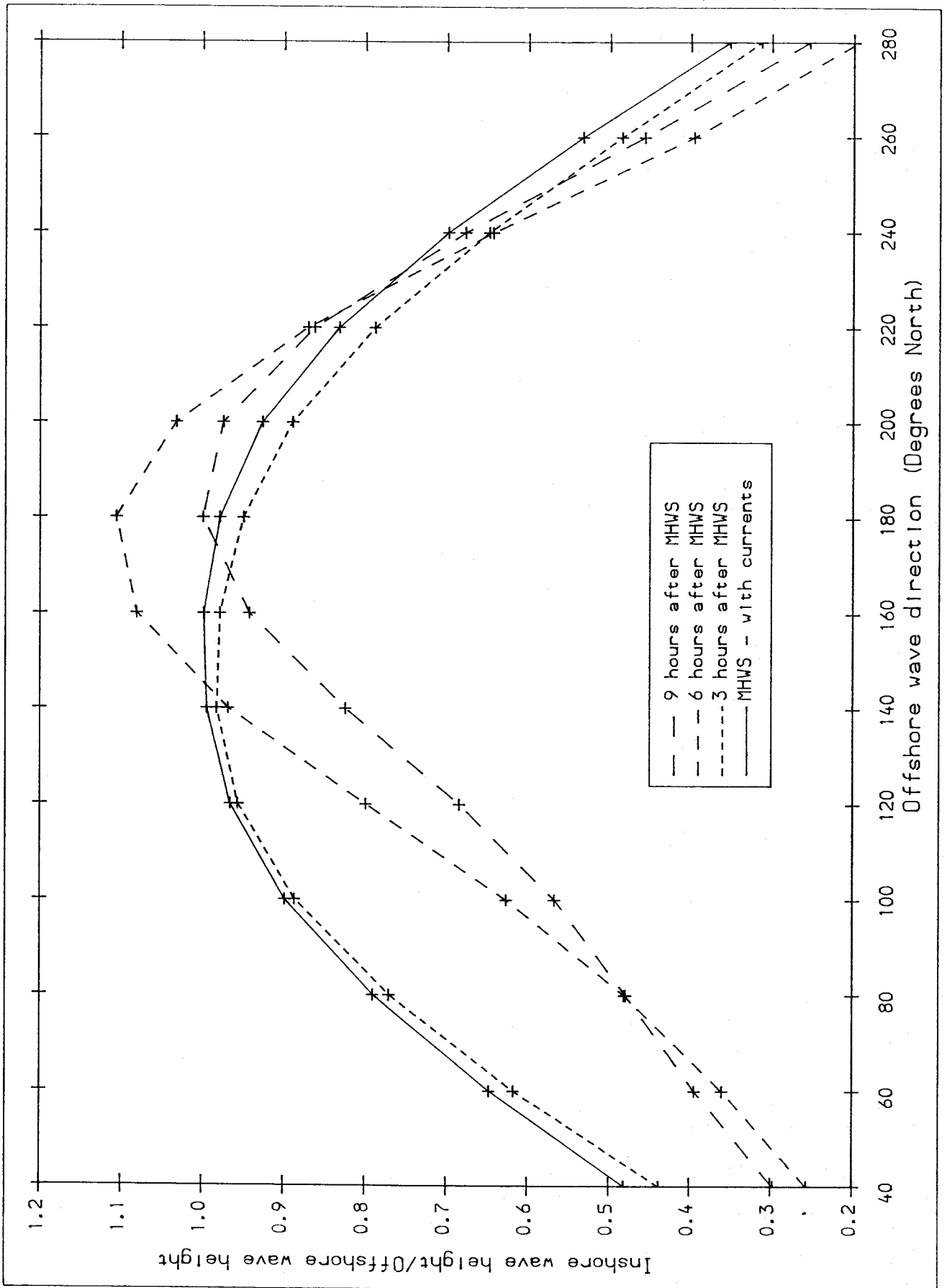


Fig 12 Wave heights from sensitivity tests - with currents

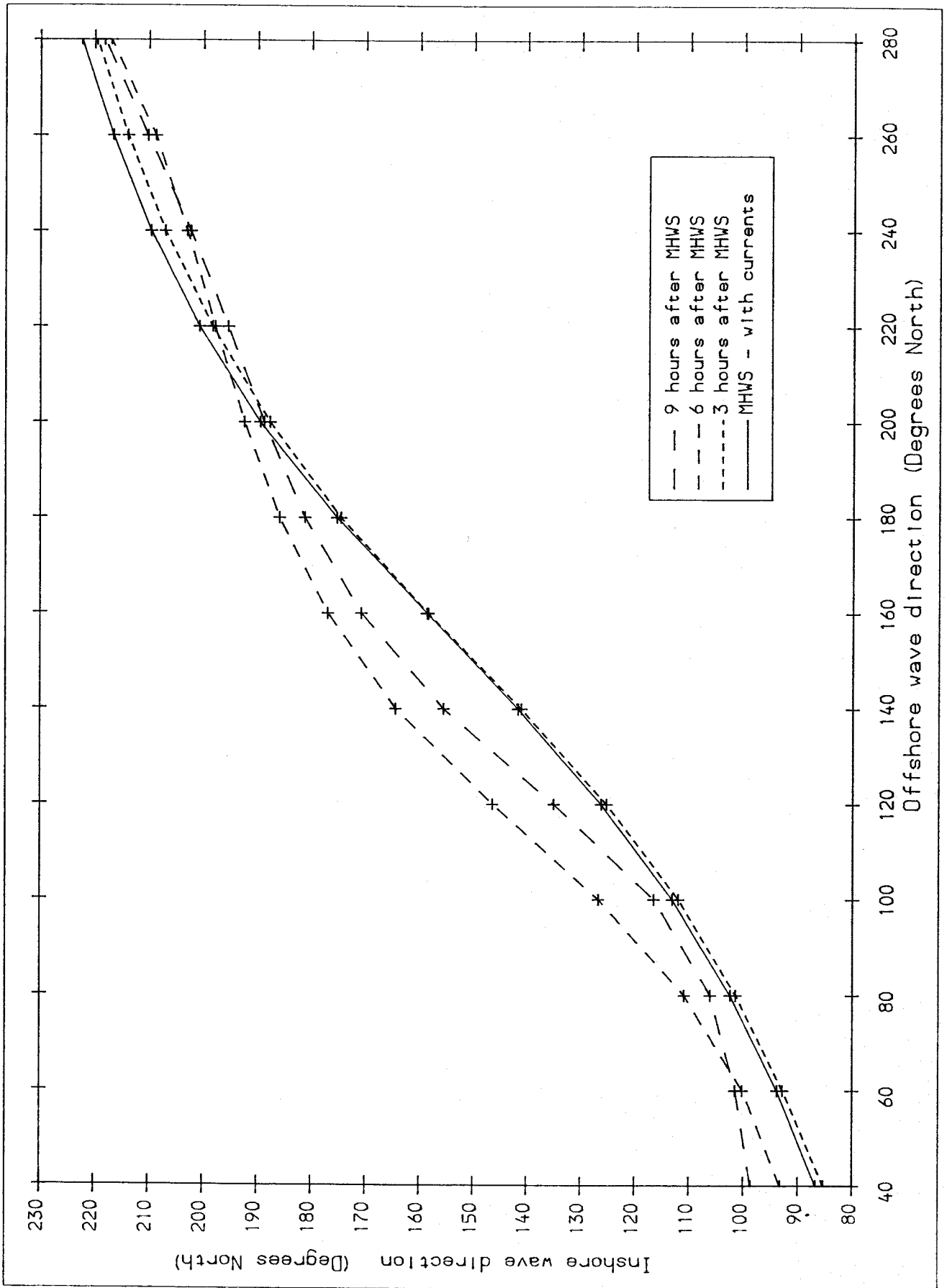
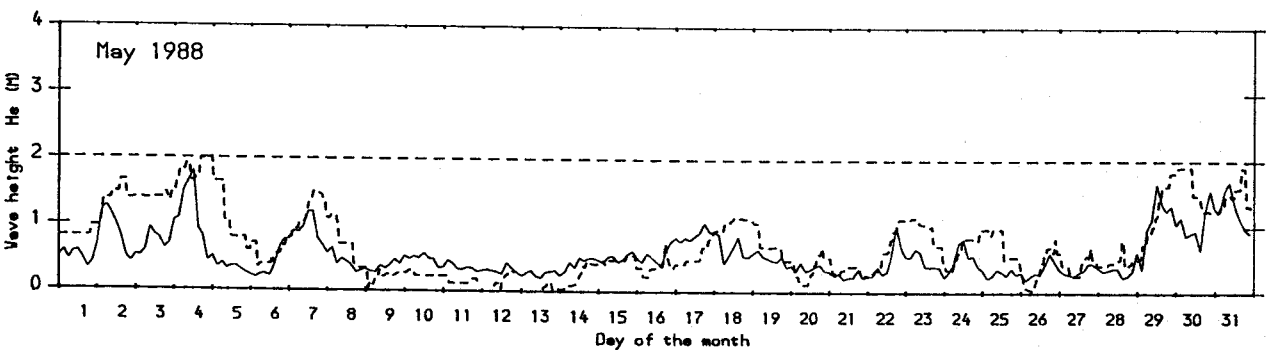
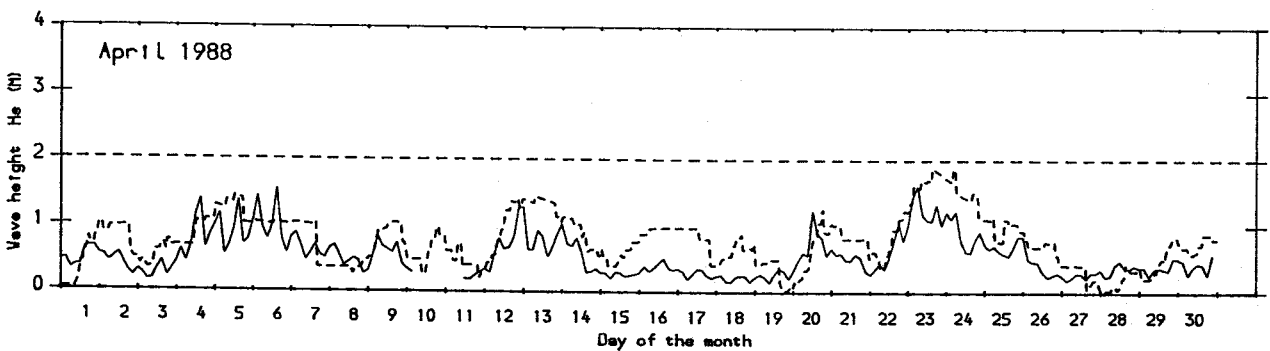
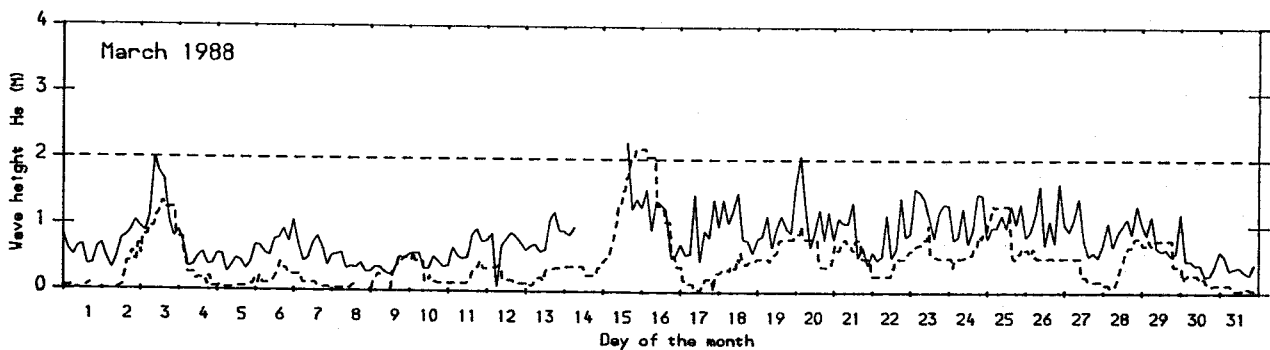
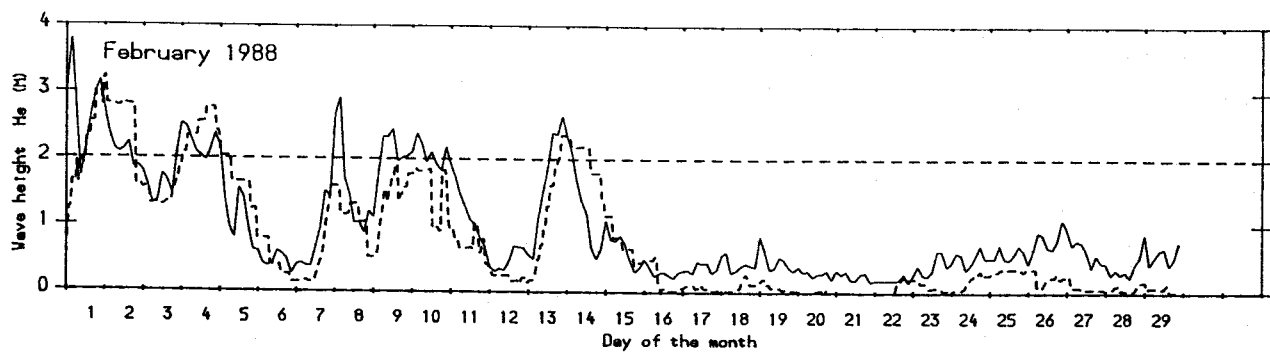
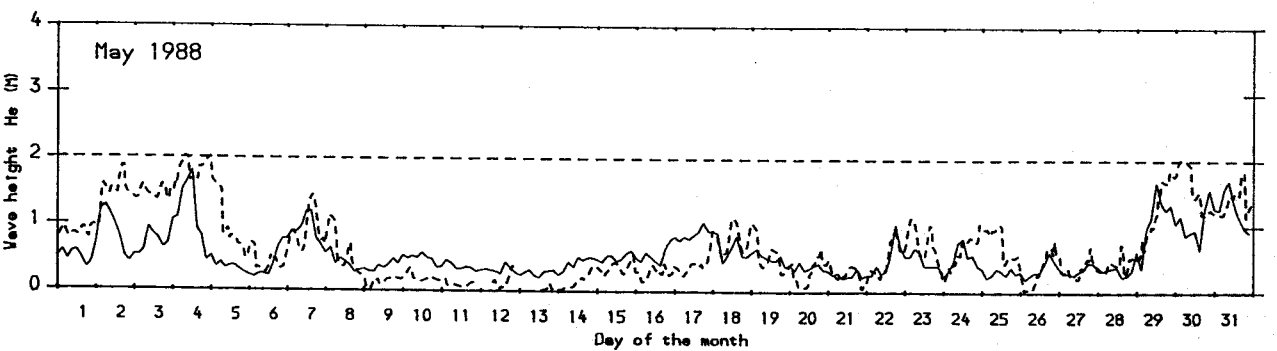
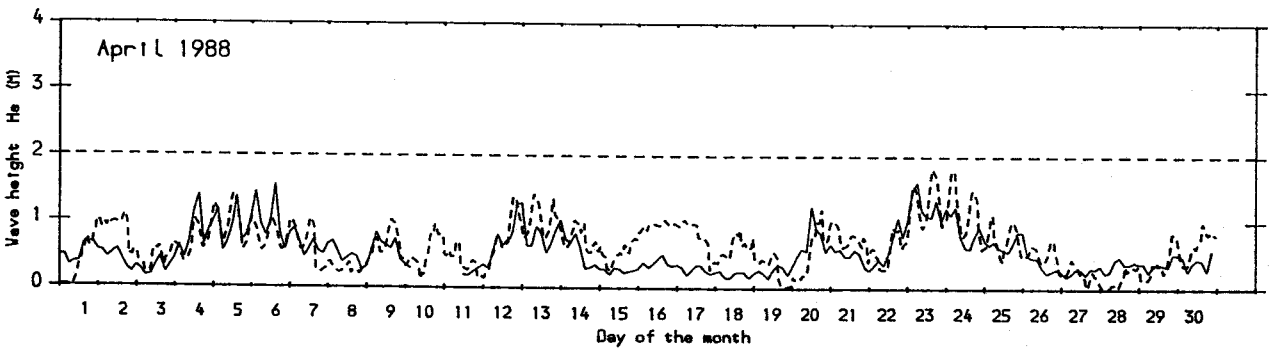
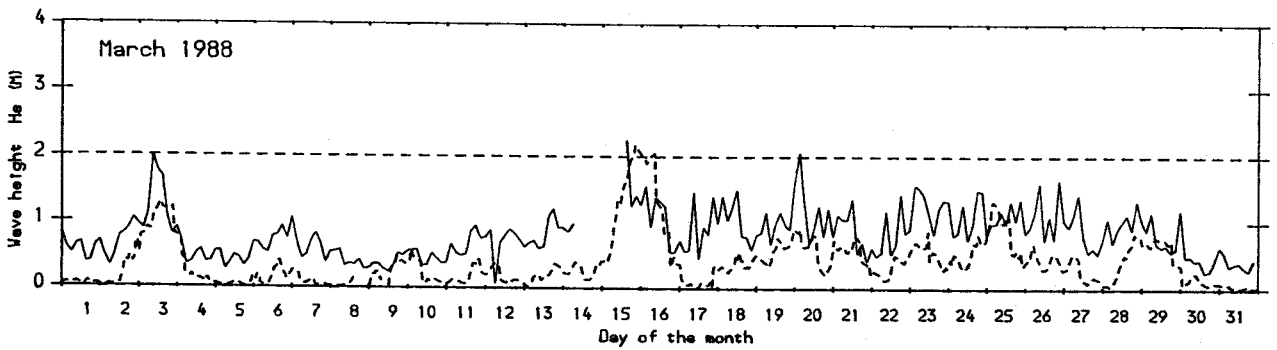
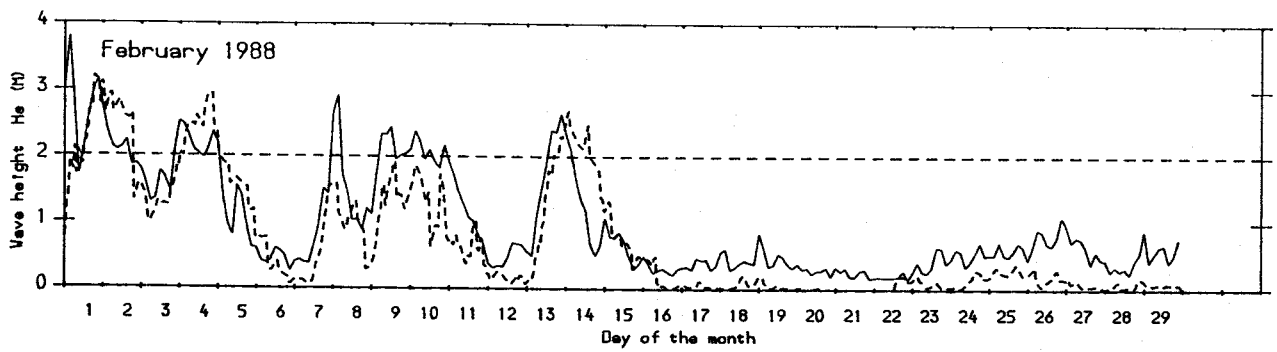


Fig 13 Directions from sensitivity tests - with currents



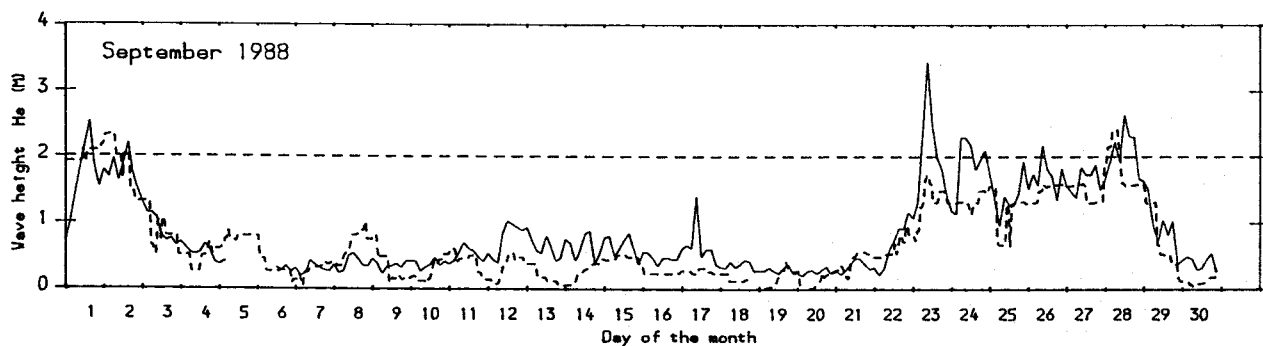
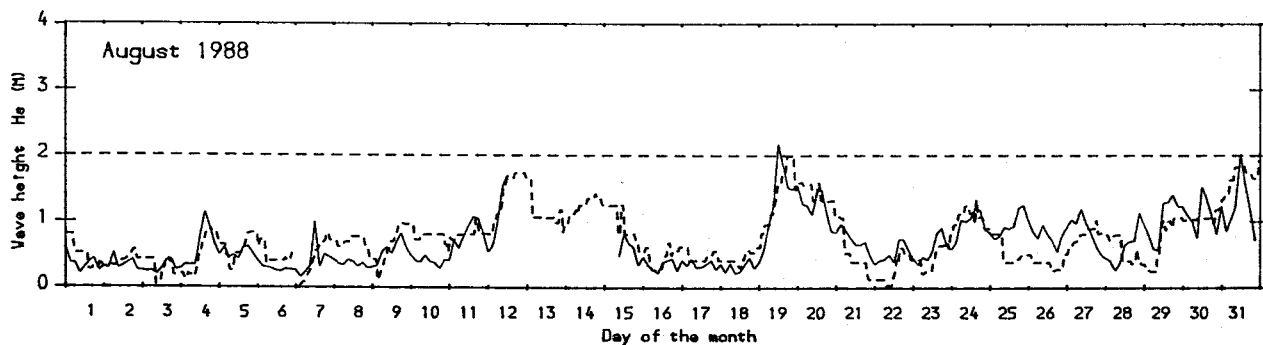
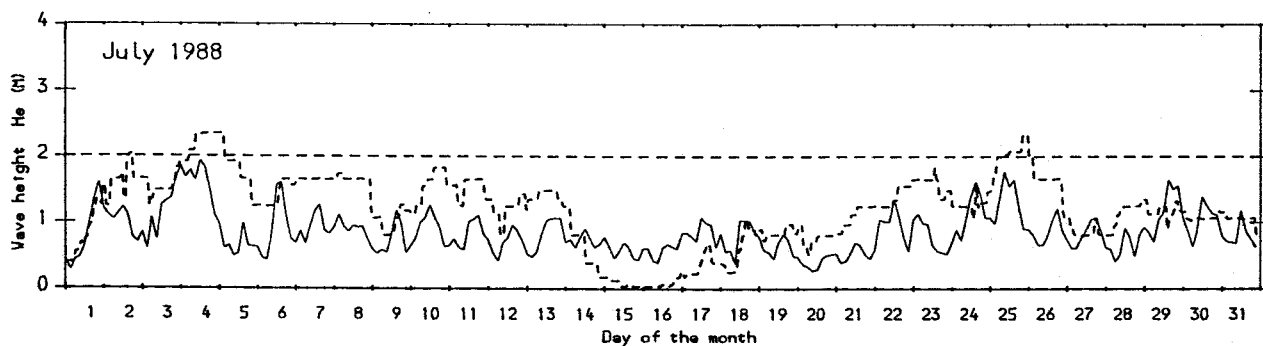
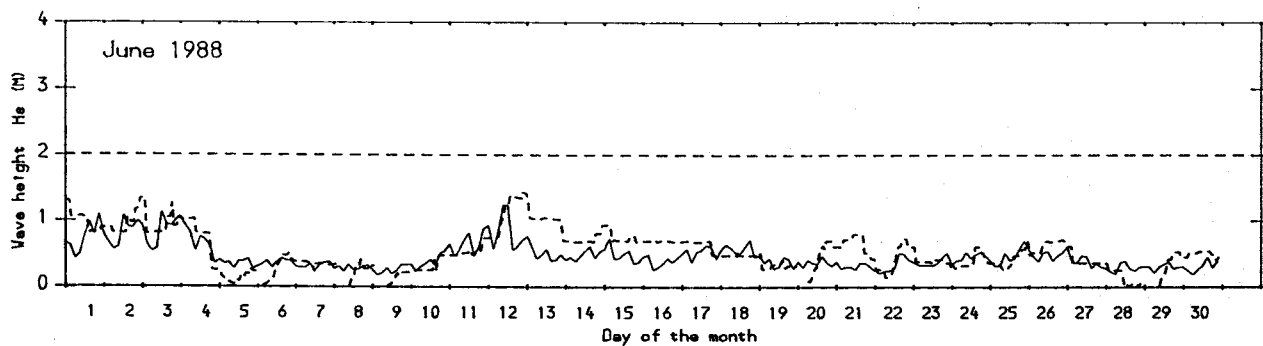
— Waves measured by a waverider buoy 1.5 Km offshore of Shakespeare Cliff
 - - - Waves predicted by the HINDWAVE/OUTURAY models at the same site

Fig 14 Wave heights for Feb to May 1988 - No currents



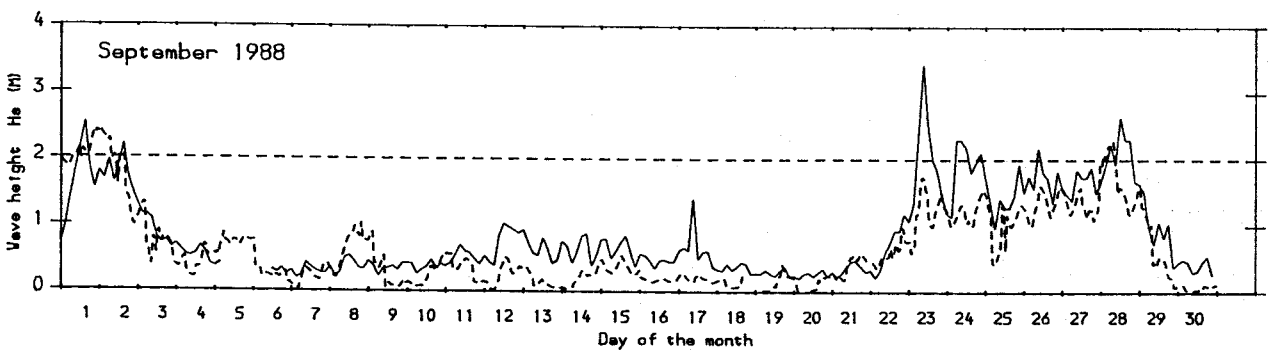
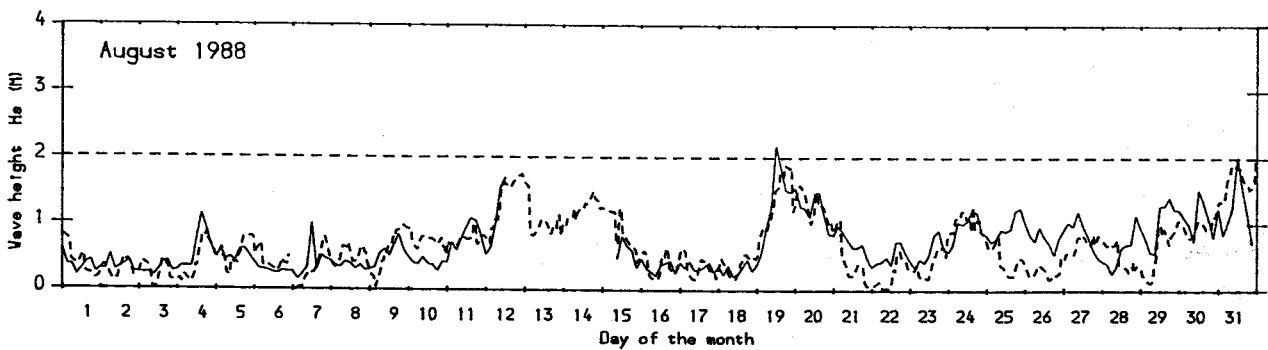
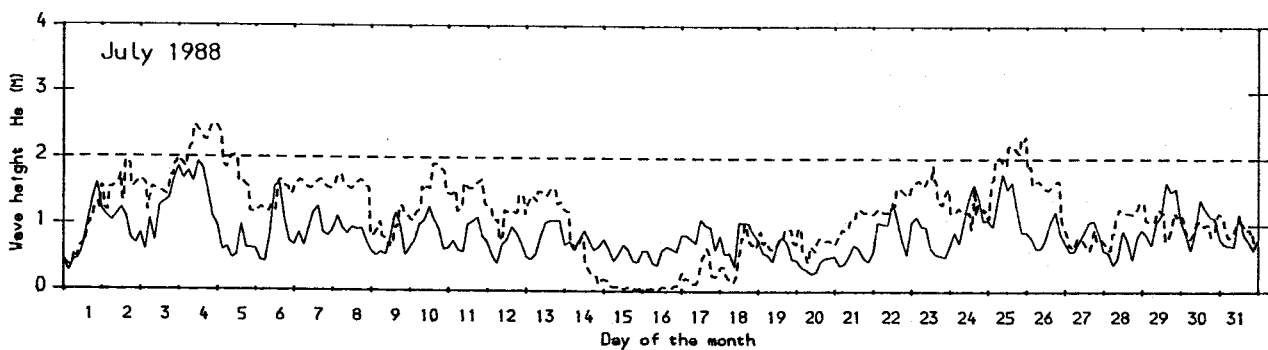
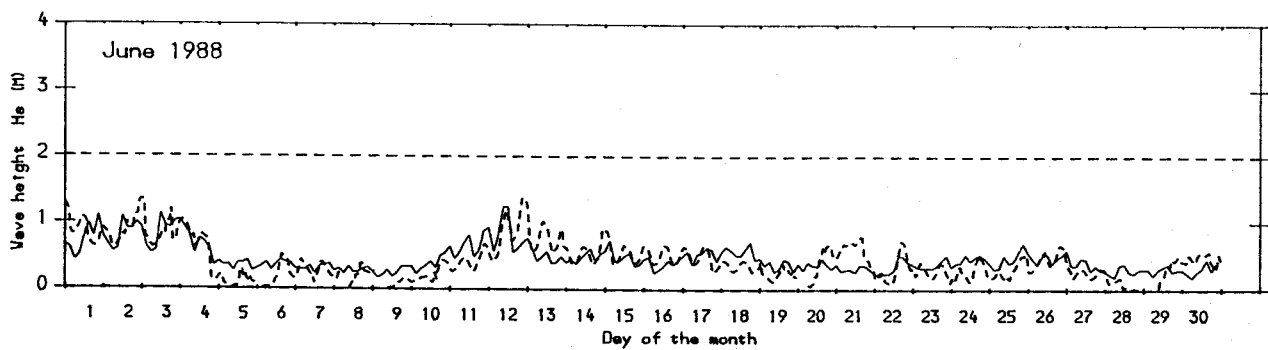
— Waves measured by a waverider buoy 1.5 Km offshore of Shakespeare Cliff
 - - - Waves predicted by the HINDWAVE/OUTURAY models at the same site

Fig 15 Wave heights for Feb to May 1988 - With currents



— Waves measured by a waverider buoy 1.5 Km offshore of Shakespeare Cliff
 - - - Waves predicted by the HINDWAVE/OUTURAY models at the same site

Fig 16 Wave heights for June to Sep 1988 - No currents



— Waves measured by a waverider buoy 1.5 Km offshore of Shakespeare Cliff
 - - - Waves predicted by the HINDWAVE/OUTURAY models at the same site

Fig 17 Wave heights for June to Sep 1988 - With currents

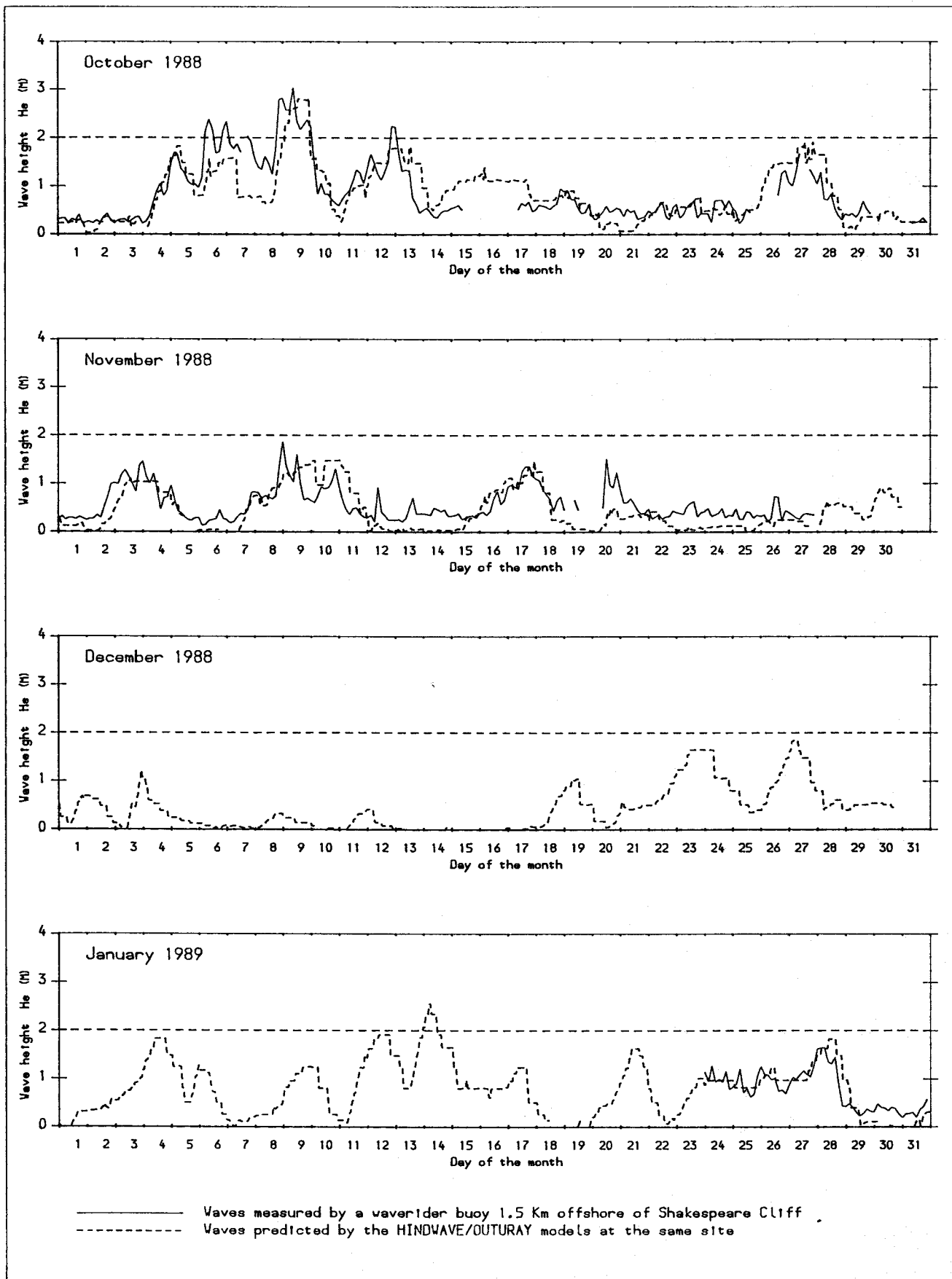


Fig 18 Wave heights for Oct 1988 to Jan 1989 - No currents

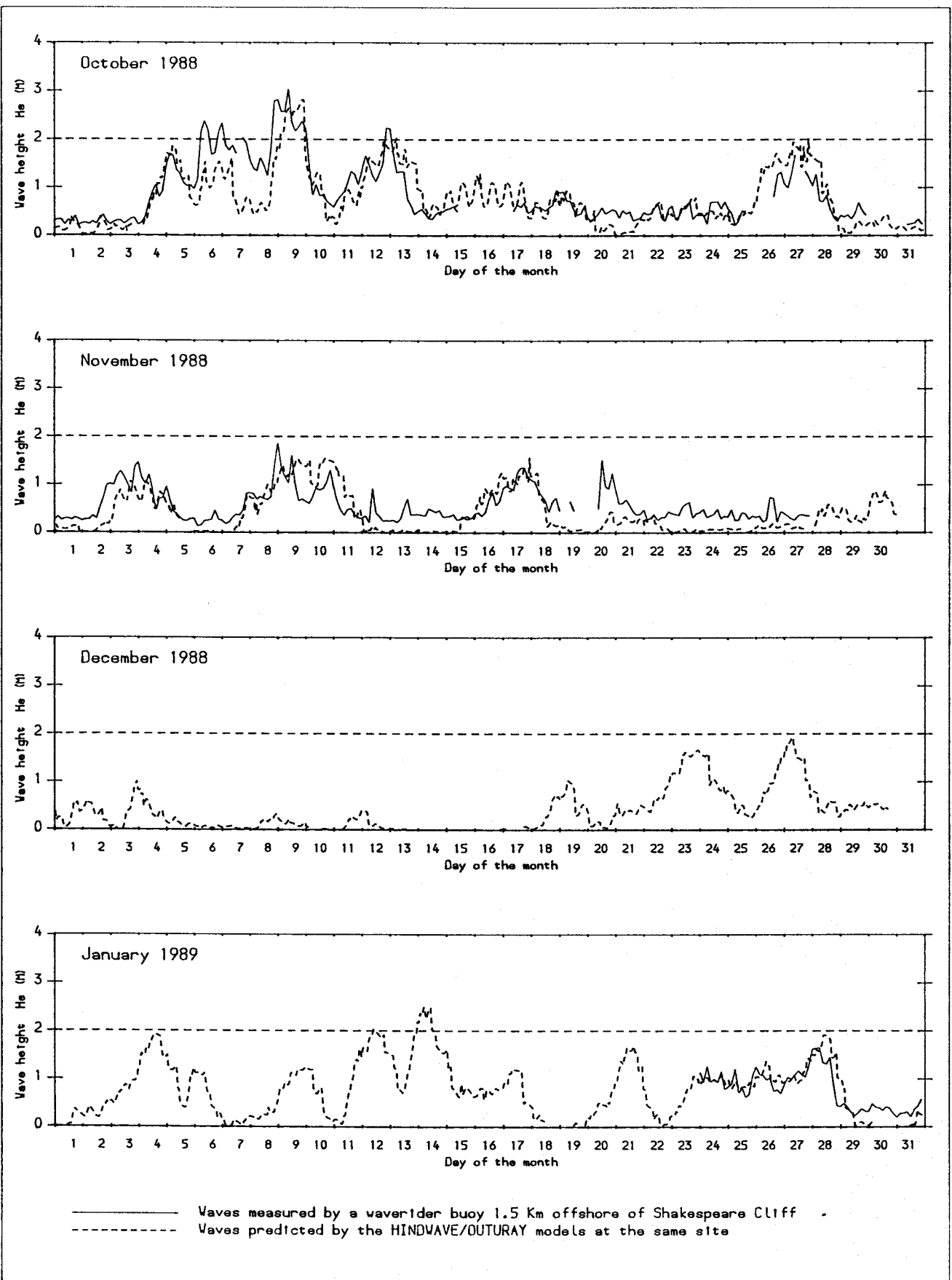
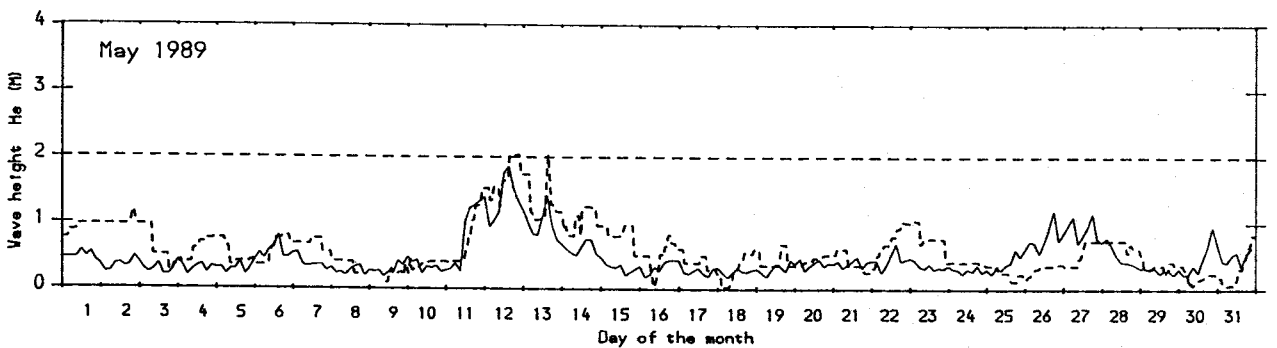
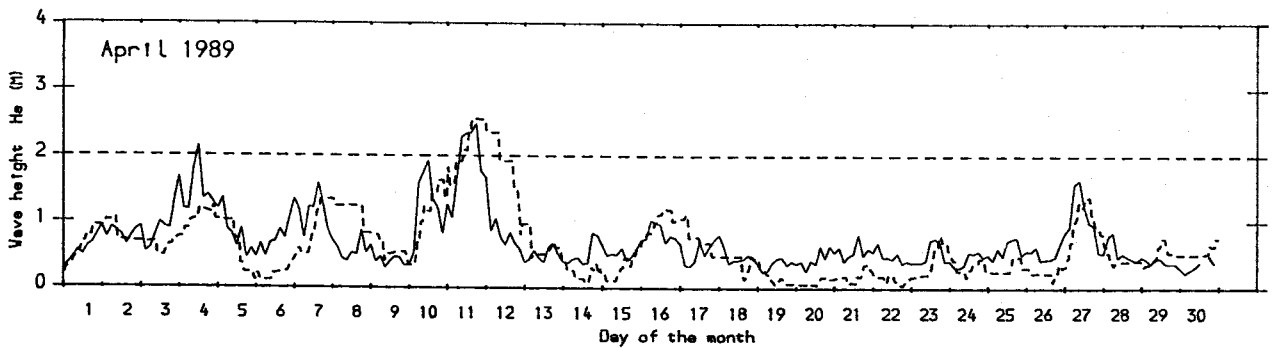
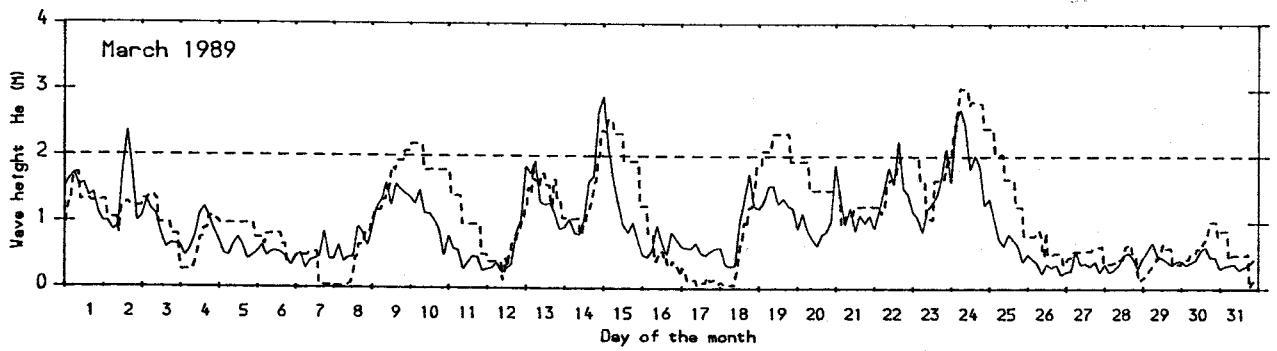
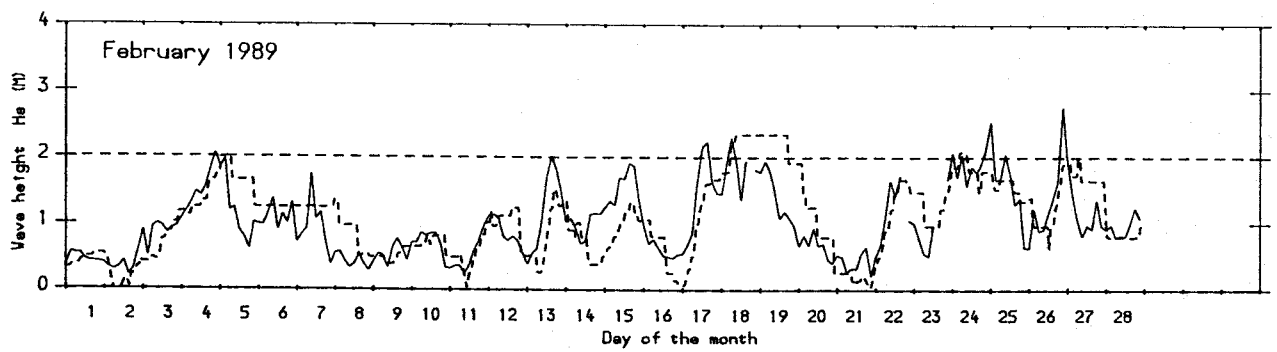


Fig 19 Wave heights for Oct 1988 to Jan 1989 - With currents



— Waves measured by a waverider buoy 1.5 Km offshore of Shakespeare Cliff
 - - - Waves predicted by the HINDWAVE/OUTURAY models at the same site

Fig 20 Wave heights for Feb to May 1989 - No currents

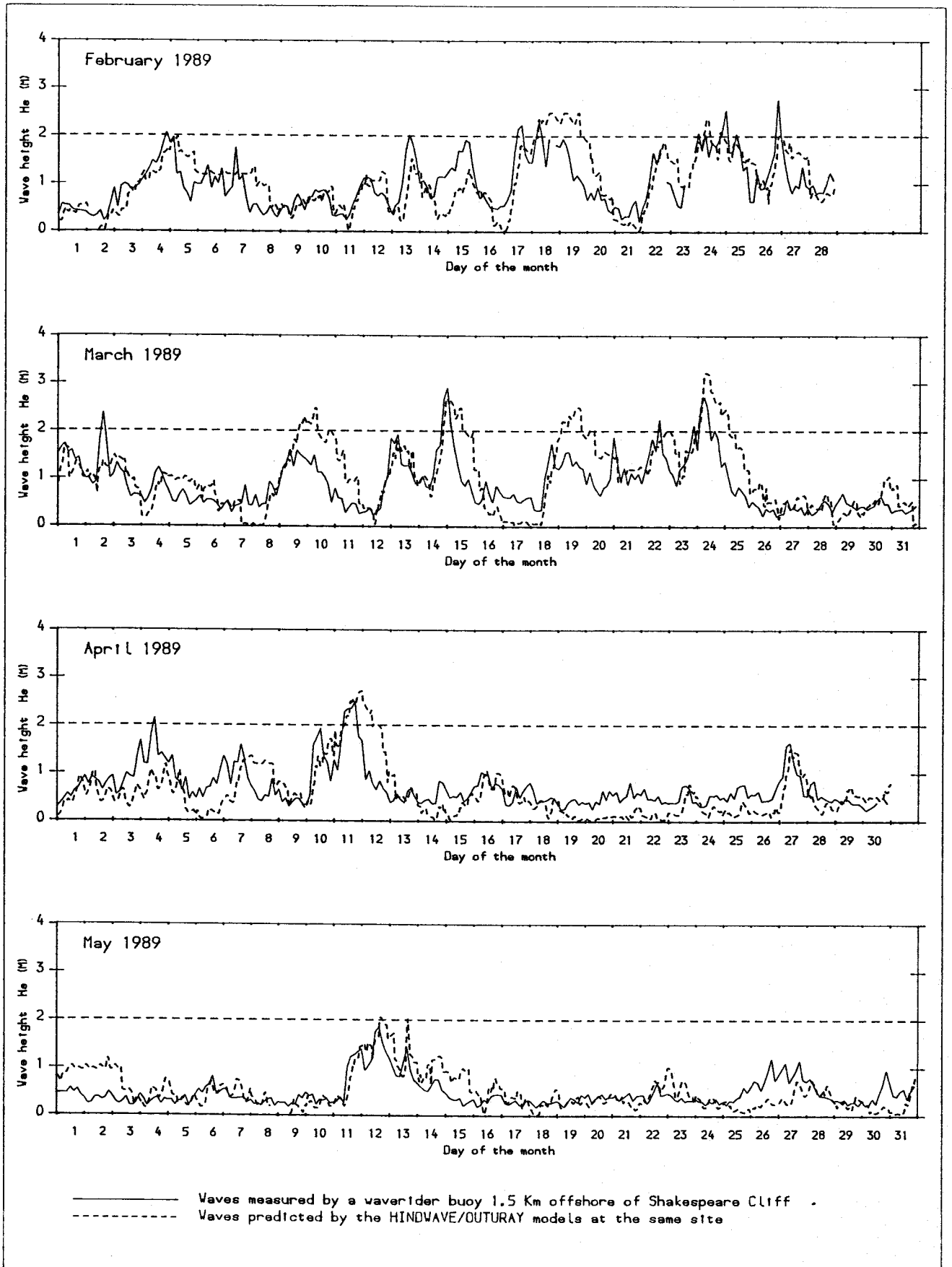
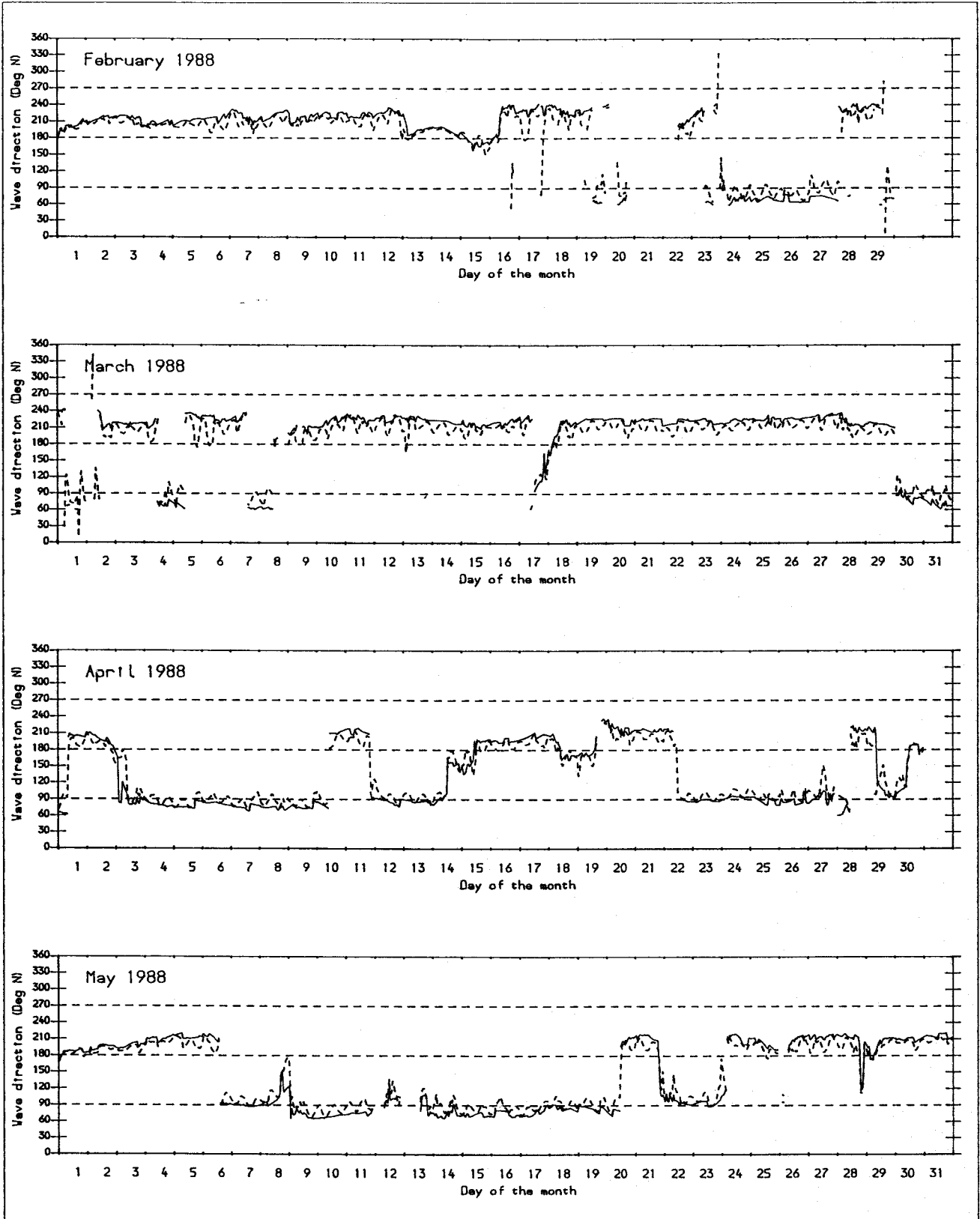


Fig 21 Wave heights for Feb to May 1989 - With currents



————— Wave directions predicted by HINDWAVE/OUTURAY ignoring currents
 - - - - - Wave directions predicted by HINDWAVE/OUTURAY including currents

Fig 22 Wave directions for Feb to May 1988

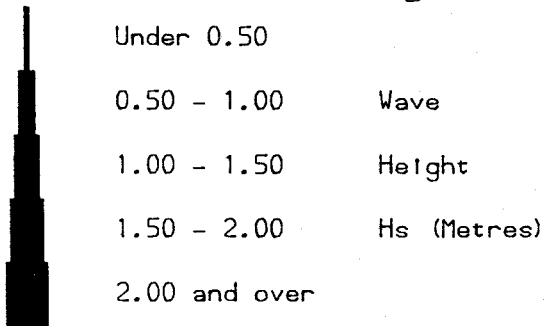
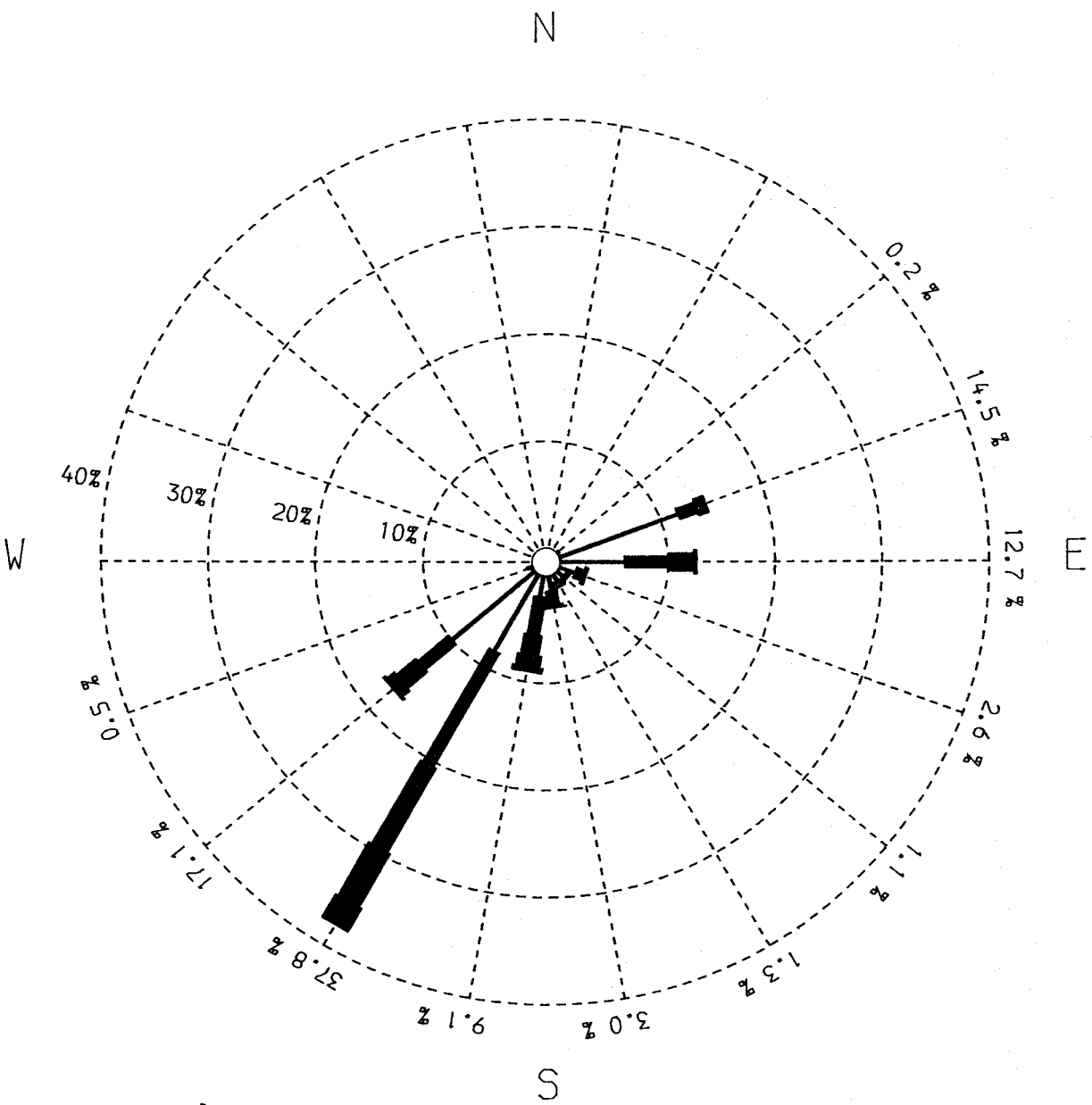


Fig 23 Inshore wave rose excluding current effects

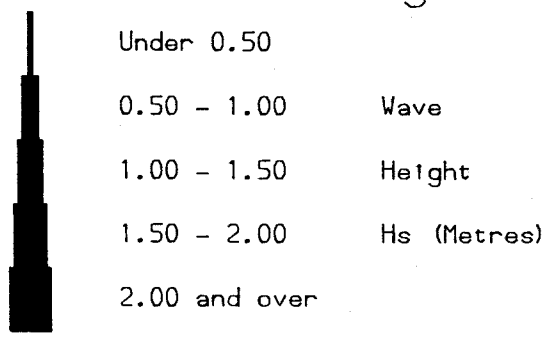
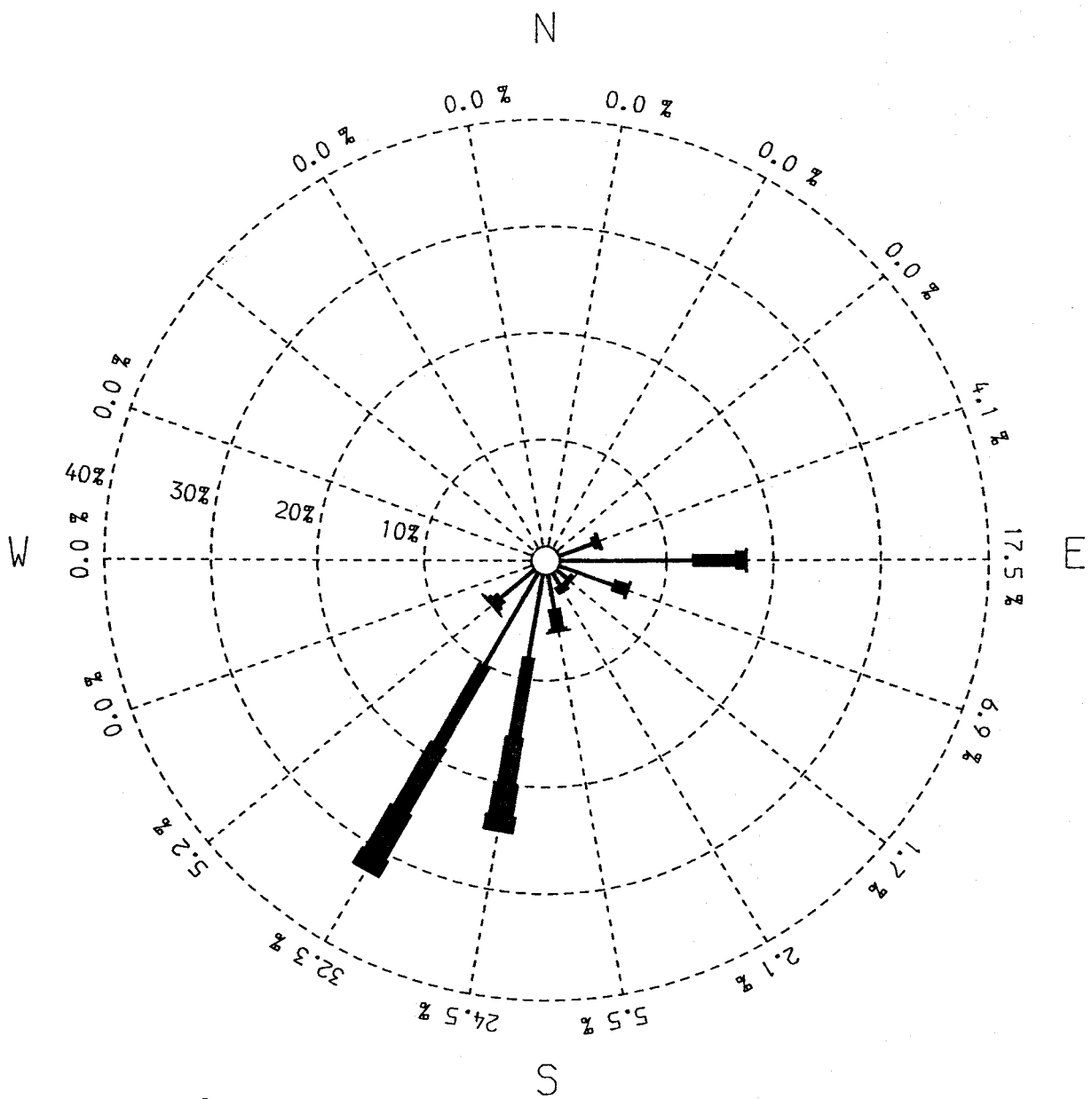


Fig 24 Inshore wave rose including current effects

——— Measured by waverider buoy
 Number of wave records is 3432 Wave records analysed from 1/2/88 TO 31/5/89
 - - - - - Predicted Ignoring currents
 Number of wave records is 9978 Wave records analysed from 1/2/88 TO 31/5/89
 - - - - - Predicted Including currents
 Number of wave records is 9983 Wave records analysed from 1/2/88 TO 31/5/89

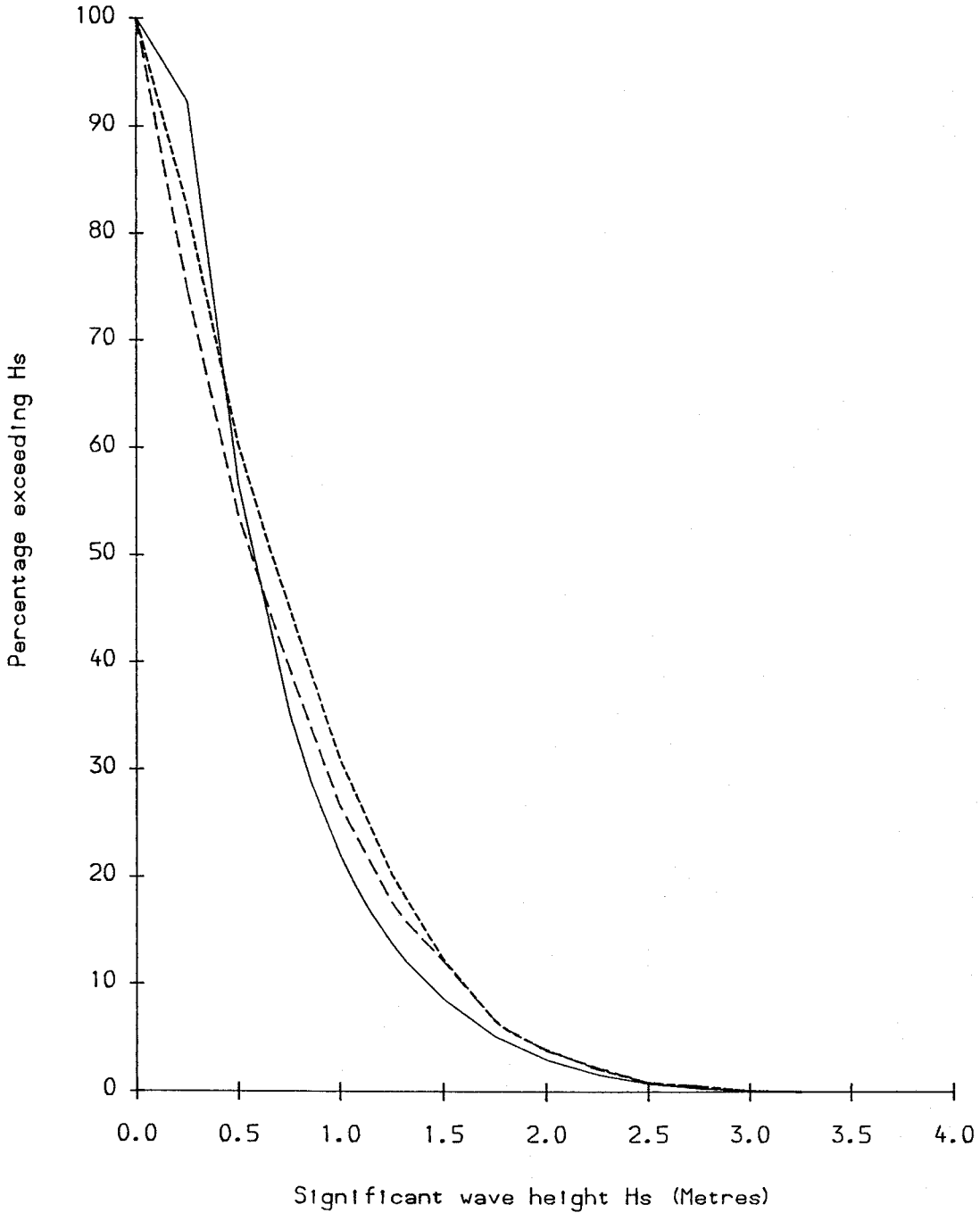


Fig 25 Wave height exceedance curve

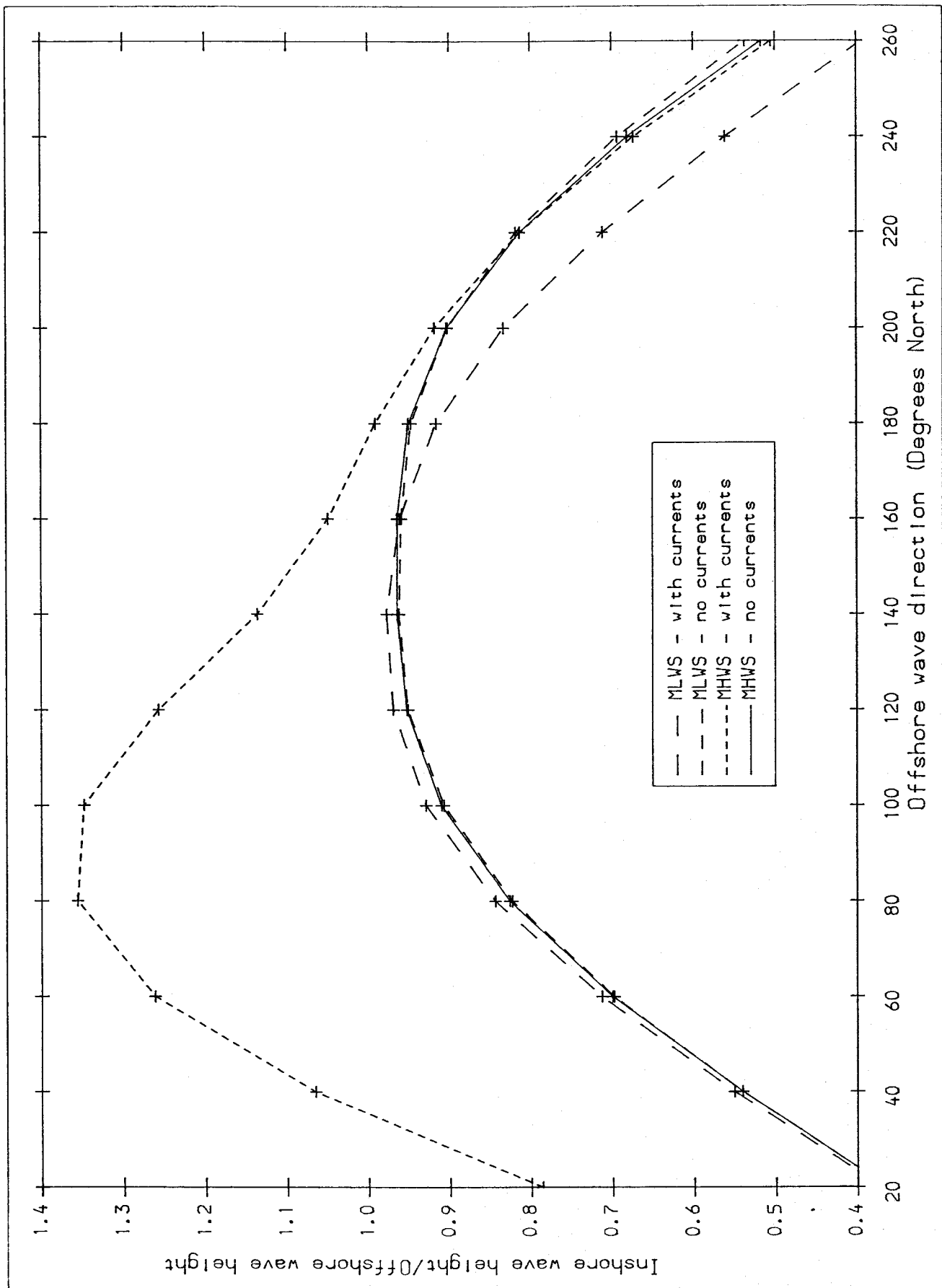


Fig 26 Wave height ratios for Point 2

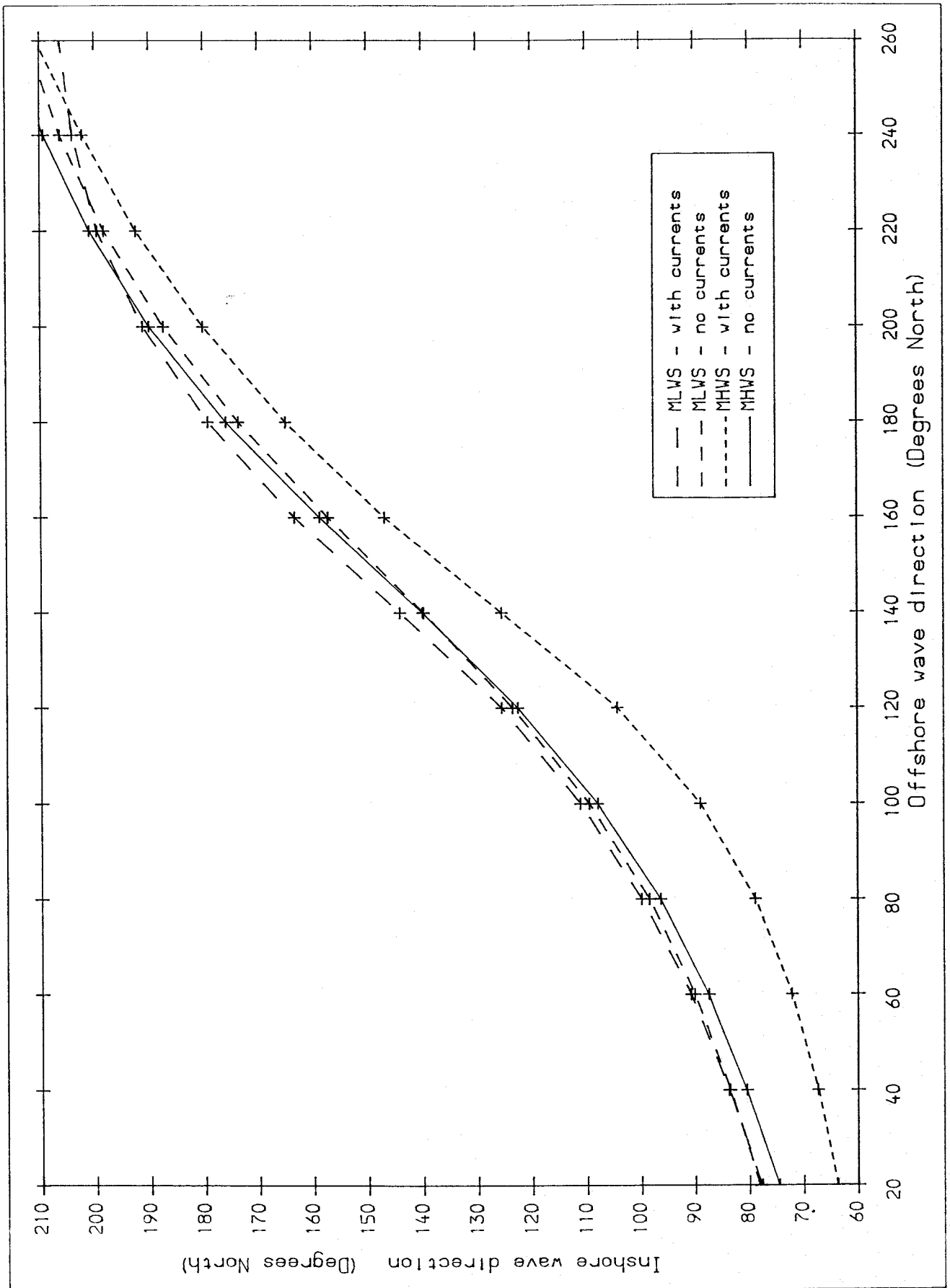


Fig 27 Wave directions for Point 2

Appendices

APPENDIX 1

The HINDWAVE wave hindcasting model

APPENDIX 1

The HINDWAVE Wave Hindcasting Model

The HINDWAVE model

The HINDWAVE model (Ref 1) has been developed at HR, for prediction of wave climate at coastal locations, based on wind records for the area. It has been used successfully on many projects at various sites around the British coast.

The computations are split into two main parts. The first stage consists of production of a menu (or list) of about one thousand possible wave conditions, from a similar number of specific wind conditions. Fetch or open water rays are measured at 10° intervals around the wave prediction point for use as input to the first element of HINDWAVE, ie the JONSEY wave generation sub-model described in Section 2 of this Appendix. The second part consists of analysis of wind records. For each hour in the sequence, the wind/wave condition most closely corresponding to actual wind activity at that time is chosen from the menu. The analysis works with measured wind data collected at hourly intervals over a period of several years. The wave conditions at any time are estimated with regard to wind speeds during the preceding day or so.

It is first necessary to define a few standard terms used in wave prediction and analysis. Significant wave height (H_s) is a parameter in common use among coastal engineers as a means of expressing wave severity. It equates to the average height of the highest one third of the waves in a sequence. Wave period is usually indicated by either mean zero-crossing period (T_z), or peak period (T_p) at which the wave energy spectrum is densest. Direction can be expressed as either wind direction (θ), or the

mean wave direction (θ_w) averaged over all frequency and direction components.

The JONSEY program is used to assign a particular H_s , T_p and θ_w to each member of a particular set of wind conditions. The set comprises all possible combinations of sufficient values of speed, direction and duration to cover the range of values expected at that location. The predicted heights, periods and directions are stored for use as a look-up table. The technique described here is to break down the measured wind data into discrete categories, and then to select the corresponding H_s , T_p and θ_w from the table.

The first stage in the procedure is to select which wind conditions could occur and to divide them into discrete bands in terms of wind speed, direction and duration. The corresponding predicted H_s , T_p and θ_w values are calculated and retained.

If the wind speed remains steady over a long period, a twenty-four hour or even longer generation time is likely to be appropriate for exposed sites. However, if the wind speed or direction is rapidly varying, a shorter duration will be used as input to the wave prediction equations. The method of selecting the duration, wind speed and wind direction for each hour, is explained below.

Hourly wind speeds and directions are obtained from the Meteorological Office in the form of a computer data file. For each hour in turn, the method determines, for the chosen group of durations, the dominant set of wind conditions at the prediction location, with reference to the H_s table. This is achieved by vectorially averaging the wind velocities over the various chosen durations leading up to that time in order to obtain an average speed and direction

for each. The largest value is then selected from the corresponding set of H_s levels. This figure is retained together with the appropriate peak period and wave direction, in order to build up a probability distribution for each month.

A further option is automatic extrapolation to extreme wave heights, for different direction sectors, based on the overall predicted distribution of H_s . This is done by fitting a three-parameter Weibull distribution to the data in each direction sector in turn, after which the results are tabulated for various return periods.

**The JONSWAP/SEYMOUR
wave prediction
model**

It is observed that wind-generated waves show some directional spreading about their mean direction of propagation. Wind travelling over a water surface transmits energy to the water in directions on either side of its own direction, which may fluctuate during the period of wave generation.

To incorporate this effect in the model, components of the total wave directional spectrum are calculated for various directions either side of the mean, and then a weighted average is taken using a standard spreading function. The significant wave height, period and direction are then calculated at the target point, by numerical integration of the spectrum.

The component directions ($i = 1$ to n) are spaced at regular intervals ($\Delta\theta$) in the range $\pm 90^\circ$ from the mean (θ_0). For each one (θ_i), the mean JONSWAP equation (Ref 2), representing a growing wind sea, is used to define the spectrum (E_i), given as a function of frequency (f):

$$E_i(f) = \alpha g^2 (2\pi)^{-4} f^{-5} \exp \{-1.25 (f/f_m)^{-4}\} \gamma^\eta \quad (1)$$

where:

$$\alpha = 0.032 (f_m U/g)^{2.3}$$

$$\gamma = 3.3$$

$$\eta = \exp \left\{ - \frac{(f - f_m)^2}{2 f_m^2 \sigma^2} \right\}$$

$$\sigma = 0.07 \text{ for } f \leq f_m$$
$$0.09 \text{ for } f \geq f_m$$

$$f_m = \text{the peak frequency (Hz)}$$
$$= 2.84g^{0.7} F^{-0.3} U^{-0.4}$$

$$U = \text{the windspeed (ms}^{-1}\text{)}$$

$$F = \text{the fetch (m) (fetch-limited conditions)}$$
$$= 0.008515t^{1.298} g^{0.298} U^{0.702} \text{ (duration-limited)}$$

$$g = \text{the acceleration due to gravity (ms}^{-2}\text{)}$$

$$t = \text{the duration (s)}$$

The summation of the component spectra is then performed using the Seymour equation (Ref 3), which includes the cosine-squared directional spreading function for a directional wave spectrum ($E(f, \theta)$). It is applied in the range $\pm 90^\circ$ from the principle wind direction. If the fetches are measured at say 10° intervals ($\Delta\theta$), then the effective wave spectrum (E) for a particular direction (θ_0) is calculated as the weighted average for seventeen component spectra ($E_i(\theta_i)$, $\theta_i = -80^\circ, -70^\circ, \dots, 80^\circ$ for $i = 1, 17$), as indicated in equation (2).

$$E = (2\Delta\theta/\pi) \sum_{i=1}^{17} E_i \cos^2(\theta_i - \theta_0) \quad (2)$$

Although it is not part of the original theory, experience at HR indicates that cosine-sixth is sometimes a better spreading function to use. This is particularly true when the wave generation area is unusually narrow or the peak period is unusually long. In order to use this modification, the cosine term in equation (2) is raised to the power six rather than two, and the coefficient $2/\pi$ is increased to $3.2/\pi$.

The significant wave height (H_s) is the average height of the largest one third of the waves. The mean zero-upcrossing period (T_z) is the period measure most frequently used in engineering, this being the average time between successive upcrossings of the mean level by the water surface. The mean wave direction (θ_w) is taken as the average of the spectral components over all frequencies and directions. They are all approximated by numerical integration of equation (2).

$$H_s = 4m_0^{1/2} \quad (3)$$

$$T_z = (m_0/m_2)^{1/2} \quad (4)$$

$$\theta_w = \theta_0 + \frac{\int \int E(f, \theta) (\theta - \theta_0) df d\theta}{\int \int E(f, \theta) df d\theta} \quad (5)$$

where $m_n = \int E(f) f^n df$

In order to use this method, fetch lengths must be known over a range of at least 180° around a point. It is convenient to use discrete frequencies in equations (1) and (2) which should also be specified.

For each application of the method, a duration and a fetch are given, although only one or other of these will produce the limiting condition used in equation (1). A complete directional spectrum is calculated, from which is obtained the one-dimensional spectrum as well as H_s , T_z and θ_w .

The directional spread of the predicted wave spectrum will generally be frequency dependent. The cosine-squared function is applied to component spectra, which are generated over different fetch lengths, and which will consequently have different total energies and different peak frequencies. This has the following realistic effect upon the calculated directional spread of energy. If the wind direction corresponds to one of the long fetch directions, then the spreading of energy at the peak will be lower than average, whilst more spreading will be observed at the highest frequencies. If the wind is blowing along one of the shorter fetches, then the spread will tend to be more even across different frequencies, and in an extreme case, may produce greater than average spreading at lower frequencies.

Appendix References

1. Hawkes P J. A wave hindcasting method. Conference on modelling the offshore environment, Society for Underwater Technology, April 1987.
2. Hasselmann K et al. Measurements of wind wave growth, swell and decay during the Joint North Sea Wave Project (JONSWAP). Deutsches Hydrographisches Institute, Hamburg, 1973.
3. Seymour R J. Estimating wave generation on restricted fetches. Proc ASCE, Vol 103, No WW2, May 1977.

APPENDIX 2

The OUTURAY wave refraction
model with currents

APPENDIX 2

The OUTURAY wave refraction model with currents

THE OUTURAY MODEL

This Appendix describes a version of the HR OUTRAY wave refraction model which includes the effects of tidal currents. In the first section the basic pure-wave OUTRAY model (without tidal currents) is described. The final section describes how the effects of tidal currents are represented in the OUTURAY model.

The basic OUTRAY model

Waves on the surface of the sea are constantly changing under the influence of a variety of external and internal forces which act simultaneously and independently. If the water is deep compared to the wavelength, the most important forces are usually the stresses resulting from wind action and internal viscosity. On the other hand, when the water becomes shallower, the effects of the seabed become increasingly important. For example, as the waves travel towards the shore they lose energy by viscous dissipation at the bed and by partial reflection, and as the water depth beneath them decreases, the waves also change direction, always tending to align their crests more nearly parallel to the contours.

This last mentioned process is known as refraction, and is similar to the refraction of light through media of different densities. The analogy can be extended further since some parts of a seabed will cause focussing of waves, whilst others will cause scattering, just as optical lenses do.

It is clear, therefore, that an accurate method predicting wave refraction is a useful design aid when

carrying out engineering studies in or beside the sea. The usual application of such a method is predicting wave conditions at a site in shallow water, either directly or in comparison with another site. Similarly it may be used to examine changes at a site that would result from altering the seabed, for example, by dredging a channel.

Since the mathematical theory of wave propagation over an irregular bathymetry is far from complete, it is necessary to make simplifying assumptions and use approximate methods. Two such assumptions are made: (1) that the waves are linear, and (2) that a wave in water of local depth, d , will behave similarly to a wave in water of constant depth, d . With these restrictions it can be shown that waves progressing over a parallel contoured seabed, change their direction according to Snell's Law, i.e:

$$C/\sin\alpha = \text{constant}$$

where α is the angle between the wave crests and the contours and where C is the wave phase speed, a function of the wave frequency, f , and the local water depth. Since the frequency of a wave remains constant, the wave direction changes only with changing depth.

The method described, like many others, relies on the concept of wave 'rays', which are lines everywhere perpendicular to the wave crests.

In order to use Snell's Law for waves proceeding over an irregular seabed, the following method is used. A lattice of triangular cells is laid over a chart of the area of interest and depth values are read off at each intersection. In each cell the seabed is then assumed to be planar, and linear interpolation is used

to define the depth at any point within the triangle. Although there is no need for the cells to be of any particular shape it is usually more convenient to choose right angled triangles which, taken in pairs, give a rectangular element.

With this representation of the seabed the depth is continuous across any grid line although the slope is usually discontinuous. It is also possible to apply Snell's Law in each cell and to follow a wave ray across it from some given entry point and direction. As the ray leaves one cell, its position and direction become the entry conditions for its journey across the next.

The time taken to calculate the ray's path across a cell can be reduced by making a further simplifying approximation. Provided the size of each cell is small and the slope of the seabed not too steep, the wave phase speed, C , at any point inside the cell can be closely approximated by linear interpolation of the exact phase speeds at the cell vertices. The ray path, under such an assumption, is part of the arc of a circle, and the path and its direction are continuous across each grid line although the curvature of the path is usually discontinuous. Because of the simplicity of the method, there are marked advantages in cost over methods which need, for example, iterative improvements at each step or more complicated representations of the seabed topography. Rounding errors can also be expected to be smaller in the described method.

The value of a wave refraction simulation, of course, lies not in the rapidity and accuracy of calculating ray paths but in the interpretation of the information they contain. Any method based on linear theory and using the concept of wave rays cannot be expected to

reproduce non-linear wave effects. In areas where the bottom topography causes strong focussing of wave rays, a situation known as a caustic, the use of linear wave theory is woefully inadequate and errors from its use will inevitably accrue. However, the method of calculating wave conditions adopted here does reduce the importance of such phenomena as caustics, and gives realistic results.

First it is assumed that in the study area a wave energy distribution $S(\theta, f, r)$ exists, where θ is the wave direction, f the wave frequency and r a position vector. In a typical open sea situation in deep water the wave energy will depend only weakly on r . On the outer boundary of the area being considered, it is thus assumed that a homogenous sea state exists and is described by $S_o(\theta, f)$, the wave energy being considered to depend solely on direction and frequency. (The subscript o is used to denote quantities at the offshore boundary).

The purpose of the wave refraction method is to provide information on the wave conditions, or energy distribution at some point P close to the shore $S_p(\theta, f)$, for a variety of offshore conditions, ie, different values of $S_o(\theta, f)$.

Suppose a ray path exists which starts from the outer boundary of the area with direction θ_o and frequency f_n and reaches the point P with direction θ_p and frequency f_n . The function S_o and S_p can then be linked by using a result of Longuet-Higgins (Appendix Ref 1), who showed that, when expressed as a function of two perpendicular wave numbers, k_1 , and k_2 , the directional spectrum $S_o(k_1, k_2)$ remains constant along a ray. So using the hypothetical ray mentioned above it can be shown that

$$S_p(\theta_p, f_n) = \mu(f_n) S_o(\theta_o, f_n) \quad (1)$$

where:

$$\mu(f_n) = (C C_g)_o / (C C_g)_p \quad (2)$$

because $S(\theta, f) df d\theta = S(k_1, k_2) dk_1 dk_2$

$$\text{and } dk_1 dk_2 = k dk d\theta = \frac{f}{C C_g} df d\theta$$

where $C = \frac{f}{k}$ the phase speed

and $C_g = \frac{df}{dk}$ the group velocity of waves.

Thus we have $C C_g S(\theta, f)$ is a constant along a wave ray, from which equation (1) follows. Provided that enough rays can be found linking the outer boundary with the point P, equation (1) can be used repeatedly to build up a picture of $S_p(\theta, f)$ for any function $S_o(\theta, f)$. All that would then be necessary are the depths at the outer boundary and the point, which would allow evaluation of C , C_g and thus $\mu(f)$.

To find such rays would be rather daunting if it were necessary to start at the outer boundary.

Fortunately, however, the paths of the rays, like those in light, are completely reversible and this makes the task very simple.

Firstly a variety of wave frequencies are chosen. For a typical study these would lie in the range 0.05Hz - 0.30Hz, and about ten would be selected. Then, for each frequency a 'fan' of rays is sent out from the point of interest. Each ray is initially separated

from its neighbour by a small angular increment, $\Delta\theta_p$; for reasons of economy the smallest separation chosen is set at $\Delta\theta_p = 0.25^\circ$, but experience has shown that larger separations can be used for the higher frequencies without affecting the results.

Each ray is 'followed', using the method described above, until it runs ashore or reaches the outer boundary. The results from this stage of the operation take the form of a list of those rays which connect the point to the boundary, with for each ray its frequency, f_n , its direction on leaving the point, θ_p , and its direction at the outer boundary, θ_o . Typically this list would contain information about several thousand rays.

For convenience this list is converted to three matrices which are called 'transfer functions', because they contain all the information necessary to evaluate the transfer of energy from the outer boundary to the point. Although it would be interesting to evaluate $S_p(\theta, f)$, the energy distribution at the point, completely, in most cases all that is required is an idea of the mean direction and directional spread of the waves together with the distribution of energy over frequency which will allow the derivation of a significant wave height and a significant wave period.

To obtain the energy for each frequency component, f_j , in $S_p(\theta, f)$ the angular dependence is integrated out. Equation (1) thus gives

$$S_p(f_j) = \int S_p(\theta_p, f_j) d\theta_p = \mu(f_j) \int S_o(\theta_o, f_j) d\theta_p \quad (3)$$

The second integral is now replaced by a summation over all those rays followed for this frequency, and so

$$S_p(f_j) = \mu(f_j) \sum S_o(\theta_o, f_j) \Delta\theta_p \quad (4)$$

where $\Delta\theta_p$ is the angular separation used at the inshore point. This summation is now simplified as follows. It is assumed that the function $S_o(\theta_o, f_j)$, is constant over angular sectors $(l-1)\Delta\theta_o$ to $l\Delta\theta_o$, $l = 1, 2, \dots, m$, with area $A_l(f_j)$ in each sector. Equation (4) becomes:

$$S_p(f_j) = \mu(f_j) (\Delta\theta_p / \Delta\theta_o) \sum_{l=1}^m A_l(f_j) \cdot N_l$$

where N_l is the number of rays with offshore direction between $(l-1)\Delta\theta_o$ and $l\Delta\theta_o$.

With the energy thus evaluated for all frequencies considered, ie f_j , $j = 1, 2, \dots, n$, the complete energy spectrum $S_p(f)$ has been approximated. Then, the significant wave height is defined as $4(\int S_p(f) df)^{1/2}$ and the zero-crossing period as $(\int S_p(f) \cdot df / \int S_p(f) \cdot f^2 \cdot df)^{1/2}$.

To obtain a mean direction and angular spread for $S_p(\theta, f)$ further investigation is necessary. We define a mean vector V at the point by

$$V(f_j) = \int S_p(\theta_p, f_j) \exp(i\theta_p) d\theta_p / \int S_p(\theta_p, f_j) d\theta_p \quad (5)$$

The mean direction θ is then given by

$$\theta(f_j) = \text{ph}(V(f_j)), \text{ the phase of } V_j$$

and the variance, or spread, $\sigma^2(f_j)$, by

$$\sigma^2(f_j) = 1 - |V(f_j)|^2$$

Following the same approximations as before, equation (5) is written

$$V(f_j) = \sum_{\ell=1}^m \frac{A_\ell}{\Delta\theta_o} \mu(f_j) \int \exp(i\theta_p) d\theta_p /$$

$$\sum_{\ell=1}^m \frac{A_\ell}{\Delta\theta_o} \mu(f_j) \int d\theta_p$$

which leads to

$$V(f_j) = \sum_{\ell=1}^m A_\ell (U_\ell + iV_\ell) / \sum_{\ell=1}^m A_\ell T_\ell$$

$$\text{where } U_\ell + iV_\ell = \mu(f_j) \frac{\Delta\theta_p}{\Delta\theta_o} \sum \exp(i\theta_p)$$

where this summation is over all the rays with offshore angle in the range $(\ell - 1) \Delta\theta_o$ to $\ell\Delta\theta_o$.

The transfer functions are thus

$$\begin{bmatrix} T_\ell \\ U_\ell \\ V_\ell \end{bmatrix} = \mu(f_j) \frac{\Delta\theta_p}{\Delta\theta_o} \sum \begin{bmatrix} 1 \\ \cos \theta_p \\ \sin \theta_p \end{bmatrix} \quad (6)$$

where the summation is over all the rays with offshore bearings in the range $(\ell - 1)\Delta\theta_o$ to $\ell\Delta\theta_o$.

We then have

$$S_p(f_j) = \sum_{\ell=1}^m A_{\ell} T_{\ell} \quad (7)$$

the mean direction

$$\theta(f_j) = \tan^{-1} \left(\frac{\sum_{\ell=1}^m A_{\ell} V_{\ell}}{\sum_{\ell=1}^m A_{\ell} U_{\ell}} \right) \quad (8)$$

and the variance

$$\sigma^2(f_j) = 1 - \left[\left(\sum_{\ell=1}^m A_{\ell} V_{\ell} \right)^2 + \left(\sum_{\ell=1}^m A_{\ell} U_{\ell} \right)^2 \right] / \left(\sum_{\ell=1}^m A_{\ell} T_{\ell} \right)^2 \quad (9)$$

As can be seen from equation (6), the functions T, U and V can be calculated simply, using information about the ray paths. It is only for substitution into equations (7), (8) and (9) that it is necessary to calculate the offshore spectrum S_o at each frequency f_j and angular sector $(\ell-1)\theta_o$ to $\Delta\theta_o$ to give A_{ℓ} .

Thus for one set of wave rays, and consequently one set of transfer functions, wave conditions at the inshore point can be calculated for a large variety of functions $S_o(\theta, f)$. The only restrictions on the offshore spectra that can be used are that they vary sufficiently slowly with θ_o that they can be assumed constant over angular sectors of width $\Delta\theta_o$ and that the frequencies f_j enable an accurate representation of the energy distribution over frequency. In practice, of course, the offshore spectra are chosen first and the quantities $\Delta\theta_o$ and f_j are then chosen to satisfy these restrictions.

Representation of
the effects of
tidal currents

The wave refraction model described above requires as input values of depth at grid intersections all over the area of interest. In addition, the wave-current model requires current magnitudes and directions to be

specified over the same grid. In principle, currents from any physical source could be included, provided they are known in advance. However, many sources of currents such as wind-generated currents, wave-induced currents, currents arising from density variations etc, are difficult to determine over wide areas. Tidal currents, on the other hand, because of their periodicity, are usually predictable over large areas even where little tidal recording has taken place. In many nearshore regions of the world, and particularly around the British Isles, tidal currents are considerably more important than currents from other sources. It was therefore envisaged that tidal currents would be the main type of current used in this model.

In selecting the current field for use in the model it should also be observed that the mathematical formulation assumes the currents to be vertically uniform and not varying with time.

To include the effects of currents in the wave refraction process requires significant changes to be made to the basic model. However, the technique of tracing rays across successive grid cells remains similar. As for the pure wave model, each grid cell is subdivided into two triangular elements, and rays are tracked across these triangles. Field quantities and their spatial derivatives are determined at any point in a triangle by linear interpolation between the field values at the three vertices. The main differences lie in the determination of the curvature of the ray paths. In the pure-wave model the interpolated quantity in each triangle is the wave celerity. With this assumption the ray curvature can be shown to be constant throughout the whole triangle. Thus the ray paths are simply circular arcs and can be determined exactly. In the wave-current model,

however, this is not the case, and the curvature of a ray path will change from point to point along the path within a triangle.

This difficulty can be overcome with an iteration process. When a ray enters a triangle, its curvature is calculated and assumed to be constant in the triangle. The exit point is determined and the curvature at that point calculated. Knowing the curvatures at the entry and exit point, an estimate can be made of the error in the ray path. If this error exceeds a certain level, the ray path is retraced using the average curvatures at the entry and exit points. This should give sufficient accuracy in most cases, but if necessary the process can be repeated further. In many instances it is found that the iteration process is unnecessary, and leads to no significant improvements in accuracy. Preliminary testing of the models before site specific runs are carried out to determine whether iterations on the ray paths are required.

The same reverse ray tracking technique is used for wave-current modelling as for the pure-wave case. For wave-current modelling the conservation of spectral density can be expressed as

$$\frac{d}{dr} \left[\frac{S(k_x, k_y)}{\omega_r} \right] = 0 \quad (10)$$

where k_x and k_y are the components of wavenumber in the co-ordinate directions and ω_r is the relative angular frequency. This condition follows from Liouville's Theorem in classical mechanics.

Since offshore spectra are usually given in terms of period (or frequency) and orthogonal angle (α), we

require the spectral density in (10) to be a function of these quantities. We can obtain the relation between the two by equating infinitesimal elements.

$$S(k_x, k_y) dk_x dk_y = S(\omega_a, \alpha) d\omega_a d\alpha \quad (11)$$

$$\text{Now } dk_x dk_y = k dk d\alpha$$

and, by differentiation of the Doppler equation,

$$d\omega_a = (c_{gr} + U \cos(\delta - \alpha)) dk,$$

where δ is the current direction

$$\text{Therefore } S(k_x, k_y) = \frac{c_{gr} + U \cos(\delta - \alpha)}{k} S(\omega_a, \alpha)$$

Substituting into (10),

$$\left(\frac{c_{gr} + U \cos(\delta - \alpha)}{k \omega_r} \right) S(\omega_a, \alpha) = \text{Constant along a ray} \quad (12)$$

The determination of the inshore spectrum and related statistical quantities is identical to the pure-wave back-tracking model. A more detailed description of the wave-current model is given in Reference 2.

Appendix References

1. Longuet-Higgins M S. The transformation of a continuous spectrum by refraction. Proc. Camb. Phil Soc, No 1, 1957, pp226-229.
2. Southgate H N. Current-depth refraction of water waves. A description and verification of three numerical models. Hydraulics Research Report SR 14, January 1985.

APPENDIX 3

Prediction of extreme wave conditions

APPENDIX 3

Prediction of Extreme Wave Conditions

There are several different methods of estimating extreme events from limited data. They are based upon the idea of fitting a standard probability distribution to the range of data which is available. The extreme wave heights are then obtained by substituting the corresponding extreme probability levels into the fitted equation.

For this approach to work properly, the data should be a representative sample, for example one year of continuous record, and not be unfairly weighted in favour of one particular time of the year. In addition, the probability theory demands that the recorded events be independent. A suitable method is to use a large number of regularly measured H_s values and to assume that the lack of independence between neighbouring values will be overcome by virtue of the volume of data involved (Ref 1).

The three-parameter Weibull distribution (Equation 1) has previously been found to be the most reliable and consistent method of fitting distributions of wave data. The parameters of the distribution are calculated after plotting the various exceedence levels on Weibull scaled graph paper (Equation 2), and drawing the best fit straight line through the points. As a check, this procedure is reproduced by a computer program and the results compared.

Extreme Value Distribution

$$P(H_s) = 1 - \exp[-\{(H_s - a)/b\}^c] \quad (1)$$

where H_s = significant wave height
 P = probability less than H_s
 a, b, c are parameters to be found

Weibull Scales

$$\log \{- \log (1-P(H_s))\} = c \{ \log (H_s - a) - \log b \} \quad (2)$$

$y = \log \{- \log (1-P(H_s))\}$ x and y are plotted
 $x = \log (H_s - a)$ on linear scales

Waves of a given return period (N years) are determined graphically from the appropriate probability. In order to calculate the correct probability, it is necessary to set the duration or persistence of the return period event. For example, if three hours were chosen (as in this study), there would be a total of 2922 three hour periods per year, and the probability of the 10 year return period event would be:-

$$P(10 \text{ year event}) = 1 - 1/(10 \times 2922)$$

$$= 0.9999658$$

Note that the expected highest individual wave (H_{\max}) in a sequence is related to H_s by the approximate formula:-

$$\frac{H_{\max}}{H_s} = \frac{(\ln N)^{1/2}}{2} \quad \text{where } N = \text{the number of waves in the sequence}$$

Reference

1. Alcock G A. Parameterizing extreme still water levels and waves in design level studies. Report 183, Institute of Oceanographic Sciences, 1984.